Results in Engineering 27 (2025) 106208

Contents lists available at ScienceDirect

Results in Engineering

journal homepage: www.sciencedirect.com/journal/results-in-engineering

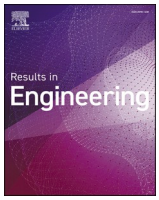

Research paper

Enhancing cementitious systems with biochar derived from invasive Prosopis juliflora

Israr Ahmad [a,b], Faheem Butt [a], Anwar Khitab [b,*]

[a] Department of Civil Engineering, University of Engineering and Technology, Taxila, Pakistan
[b] Department of Civil Engineering, Mirpur University of Science and Technology (MUST), Mirpur 10250, (AJ&K), Pakistan

ARTICLE INFO

Keywords:
Carbon-negative mortars
Prosopis juliflora biochar
Pore-refinement
Densification
Durability

ABSTRACT

Cement production significantly contributes to global CO_2 emissions, necessitating sustainable strategies that enhance performance without increasing environmental impact. This study explores the use of biochar derived from Prosopis Juliflora, an invasive plant species, as a sustainable additive in cement mortar. Produced through pyrolysis under limited oxygen, the biochar retained 83 % stable carbon, indicating its potential for long-term carbon sequestration. Various dosages (0, 0.05 %, 0.1 %, 0.15 %, and 0.2 % by cement weight) were tested over 90 days to assess mechanical, physical, and durability properties. The 0.1 % biochar dosage showed optimal performance, increasing compressive strength by 11.5 %, flexural strength by 21 %, and density by 3.5 %, while reducing porosity by 21 % compared to the control. XRD and carbonation tests revealed reduced calcium carbonate formation and improved carbonation resistance. Freeze-thaw tests showed enhanced durability due to reduced permeability, while thermal tests indicated that low-dose biochar acts as a dehydration promoter, and at higher dosages, as a thermal insulator. At elevated temperatures, biochar's porous structure released internal steam, minimizing microcracking and preserving strength. Improved residual bending strength at high temperatures was attributed to the crack-bridging effect of biochar. These benefits are linked to the densification and pore refinement of the cement matrix without increasing cement content. Utilizing an invasive species adds ecological value, aligning with circular economy principles. This research highlights biochar as a promising, waste-derived alternative to conventional additives, offering a dual advantage of enhancing mortar performance and reducing the construction sector's carbon footprint.

1. Introduction

Climate change is significantly impacting the Earth's atmosphere, prompting global efforts to achieve development with minimal environmental harm. As a major contributor to greenhouse gas emissions, the construction industry is actively seeking sustainable alternatives to conventional materials. Cement, a key component in infrastructure such as buildings, roads, dams, and bridges is the second most consumed substance globally after water [1]. Its large-scale production, exceeding 3 billion tons annually [2], is energy-intensive and responsible for considerable CO_2 emissions, estimated at 600–800 kg per ton of cement produced. To align with the Net Zero Emissions (NZE) scenario by 2050, a 4 % reduction in cement-related emissions is required by 2030 [3]. To address this challenge, researchers have explored various supplementary cementitious materials, including silica fume, fly ash, and blast furnace slag, which improve fresh and hardened properties while reducing cement content [4–7].

In this context, biochar has emerged as a novel and environmentally beneficial additive in cementitious systems. Derived from biomass through pyrolysis under limited oxygen supply, biochar is a carbon-rich, porous material characterized by high surface area, alkalinity, and moisture retention capacity [8,9]. While historically used in agriculture to improve soil fertility, recent research has highlighted its potential in construction materials [10–12]. Biochar can serve as a partial cement replacement or micro-filler, contributing to carbon sequestration and enhancing internal curing, shrinkage resistance, and long-term durability. Moreover, it can influence hydration kinetics and microstructural development, ultimately improving the mechanical performance of cement-based composites [13]. Its effectiveness, however, depends on factors such as feedstock type, pyrolysis temperature, particle size, and dosage [14]. As such, integrating biochar offers a dual advantage of reducing the environmental footprint of cement while enhancing

* Corresponding author.
E-mail address: anwar.ce@must.edu.pk (A. Khitab).

https://doi.org/10.1016/j.rineng.2025.106208
Received 19 April 2025; Received in revised form 2 July 2025; Accepted 8 July 2025
Available online 9 July 2025

material performance.

Despite growing interest, the application of biochar in cementitious composites such as concrete and mortar remains a relatively new but rapidly developing research area [15–17]. Its high carbon content enables effective long-term carbon sequestration, aligning with global efforts to curb greenhouse gas emissions. Given the increasing global use of cement-based materials and the associated rise in carbon footprint, integrating biochar into these systems offers a viable route to reduce cement demand while enhancing key performance metrics such as strength and durability [18,19]. Biochar is typically derived from pyrolyzing biomass wastes, including household, industrial, and agricultural residues that are otherwise landfilled or openly burned [20]. When subjected to pyrolysis at temperatures exceeding 500 °C, volatile organic compounds are released, yielding a lightweight, porous material with distinct physico-chemical characteristics [21]. This porous structure supports internal water retention, which can enhance hydration and improve the long-term durability of cement composites [22]. Studies have demonstrated that the incorporation of biochar, either as a cement substitute or as an additive can result in measurable benefits across both environmental and mechanical dimensions of cementitious materials [23]. Biochar enhances the crack resistance of cementitious composites through several synergistic mechanisms. Its fine particles act as nano-reinforcements, filling micro-pores and densifying the matrix, thereby limiting crack initiation [24]. The material's intrinsic porosity aids in absorbing excess water [25], which may reduce shrinkage-induced cracking while supporting continued hydration. In the event of microcrack formation, biochar particles can bridge the cracks, deflecting and redistributing stress to slow or prevent further propagation [26]. Moreover, biochar's high surface area improves bonding within the interfacial transition zone (ITZ), enhancing fracture energy dissipation [27]. By refining the pore structure and increasing overall toughness, biochar contributes to a more ductile matrix capable of resisting both static and dynamic cracking, ultimately boosting the durability and mechanical performance of cementitious materials. These microstructural and mechanical enhancements attributed to biochar have also been supported by experimental findings in many recent studies.

According to Gupta et al., porous and ridged shaped structure of biochar improves bonding with cement paste. It was also highlighted that porous biochar absorbs water during concrete mix which reduces amount of free water in matrix [28]. Choi et al. studied the effect of biochar extracted from switchgrass and hardwood on properties of mortar. Replacing 5 % cement with biochar increased compressive strength by 10 % after 28 days of curing. The authors also observed that samples containing biochar required more amount of water due to porous nature of biochar [29]. Gupta et al. replaced 2 % mass of cement with biochar made from mixed wood and reported 40 % increase in strength of concrete samples on 7th day of curing [30]. Sirico et al. reported increase in compressive strength when 5 % cement was replaced with biochar made of wood waste [31]. Park et al. used oilseed rape and mixed softwood biochar in mortar. The authors used varying quantities of biochar from 2 to 8 %. The highest compressive strength was achieved on using 4 % biochar with respect to weight of cement irrespective of the type of biochar used [18]. Kim et al. utilized biochar derived from spruce trees, rice husks, and miscanthus straw. Their findings revealed that incorporating 6 % biochar led to a reduction in the strength of the specimens. However, specimens containing 4 % biochar exhibited comparable or even improved strength. Additionally, thermal conductivity decreased with increasing biochar content, and the inclusion of 6 % biochar lowered the peak temperature of the specimens by 4–5 °C [32]. Gupta et al. prepared biochar from rice husk and waste wood. 1–2 wt% of rice husk biochar and waste wood biochar reduced water permeability in comparison with control [33]. Tayyab et al. used biochar of millet and maize in a percentage of 0.025–1 % by mass of cement in mortar specimens. Their findings revealed that the biochar enhanced mechanical strength, toughness, and reduced porosity. The optimum addition of millet and maize has been reported as 0.2 and 0.5 % respectively [34]. Iftikhar et al. used biochar of bagasse and pine needles. The proportions varied from 0.025–1 % by mass of cement in mortars. It was reported that the toughness and electromagnetic shielding were much improved with the addition of biochar [35]. The characteristics of biochar depend on the feed stock from which it is produced. According to Mensah et al. properties of biochar depend on temperature as well as type of biomass [36]. The type of biochar and its production conditions affect the properties of cement composites. For example, in a research study, it was concluded that biochar produced from barley straw showed more improvement in compressive strength of concrete in comparison with biochar produced from manure [37]. Research conducted by Gupta and Kua showed that biochar produced at high pyrolysis temperature gave more compressive strength to mortar in comparison with biochar produced at low temperature [30].

While a growing body of research has explored the incorporation of biochar from various biomass sources, such as rice husk, wood waste, switchgrass, barley straw, millet, maize, and bagasse into cementitious materials, no prior study has focused specifically on the use of Prosopis juliflora biochar in this context. This research uniquely addresses a dual challenge: the utilization of a highly invasive and environmentally problematic species, and the development of sustainable, high-performance cementitious composites. P. juliflora, commonly known as mesquite, is an evergreen plant native to Central and northern South America [38]. It was later introduced in various regions, including Africa, Australia, and the Indo-Pak subcontinent, for purposes such as providing shade, timber, food, and soil stabilization. However, it has since become a severe ecological threat, occupying millions of hectares of land and ranking among the 100 most invasive species globally [39–41]. The plant grows aggressively, spreads rapidly, and is difficult to control. Its disposal also poses challenges, as burning contributes to air pollution while dumping may facilitate its further spread. Although ashes derived from P. juliflora have been previously used to improve soil properties [42] and enhance the performance of cementitious materials [43], the use of biochar derived from this species as an additive in mortar is entirely novel. This study proposes a sustainable solution by converting P. juliflora biomass into biochar and incorporating it into cement-sand mortar in micro- and nano-sized forms. By doing so, it not only offers a valorisation route for a harmful and underutilized biomass but also contributes to the development of eco-efficient construction materials. The research evaluates the effects of P. juliflora biochar on mortar density, porosity, compressive strength, and flexural strength, filling a notable gap in current literature and offering new insights for future applications. The present research indicates that P. juliflora biochar offers a unique combination of high carbon content, moderate extraction temperature, and sustainable sourcing, making it a competitive, eco-friendly additive for cementitious composites within a circular economy framework.

2. Materials and methods

2.1. Materials

The branches of P. Juliflora were collected from nearby fields, cut into small pieces, washed, and left to dry under the sun. The P. Juliflora in natural habitat and its oven dried form are shown in Fig. 1.

Grade C-53 cement was used in this study. The chemical composition of the cement is presented in Table 1, while its physical properties are detailed in Table 2. Grade 53 cement was chosen due to its extensive use in national construction projects.

Natural river sand sourced from Lawrencepur was used as the fine aggregate. The physical properties of the sand are summarized in Table 3.

Biochar absorbs water and reduces flow [29], which can significantly impact the workability of concrete mixes. To address this issue and ensure proper consistency, a water-reducing admixture was

Fig. 1. Stages of biomass preparation: (Left) P. Juliflora plant in its natural habitat. (Right) Oven-dried P. Juliflora plant ready for pyrolysis.

Table 1
Chemical composition of grade 53 cement (% by weight).

Composition	Lime	Silica	Aluminum Oxide	Magnesium Oxide	Iron Oxide
Content (%)	65	19	4.97	2.23	3.27

Table 2
Physical properties of grade 53 cement: key performance metrics.

Property	Surface area (cm^2/g)	Density (g/cm^3)	Normal consistency (%)	Initial setting time (hr)	Final setting time (hr)
Measured value	3200	3.15	27	0.5	10

Table 3
Physical properties of Lawrencepur river sand.

Property	Specific gravity	Bulk density (Kg/m3)	Water absorption (%)
Measured value	2.71	1495	2.8

incorporated into the mix.

The pyrolysis of biomass (P. Juliflora) was conducted in a tube furnace with a length of 6000 mm and a diameter of 60 mm. The furnace was equipped with dual heating chambers, each having a length of 300 mm. Inert gas (Argon) was introduced into the system through a cylinder connected to the tube. For each pyrolysis cycle, a 50-g sample of biomass was placed inside the tube, as shown in Fig. 2.

Pyrolysis was carried out at 600 °C with a heating ramp of 20 °C per minute until the temperature reached 600 °C. Once the desired temperature was achieved, it was maintained at 600 °C for 30 min to ensure complete thermal decomposition of the biomass. After this period, the temperature gradually reduced over the course of one hour until it returned to room temperature. The flow of Argon was continuously maintained at 80 mL/min to create an inert atmosphere during the process. The blackish material produced through pyrolysis is shown in Fig. 3 (on left). This material was then subjected to ball milling at a speed of 50 rpm to reduce it to micro- and nanoscale particles. The fine biochar obtained from this milling process is depicted in Fig. 3 (on right). The yield of biochar, calculated based on dry biochar, was 33 %.

For the sake of comparison, the biochar of P. Juliflora is compared with the other compatible biochars in Table 4.

The biochar derived from Prosopis Juliflora at 600 °C demonstrates exceptional carbon retention (83 %), rivaling high-performance feedstocks like Cono carpus wastes (84.97 % at 800 °C) and mixed wood (87.13 % at 500 °C), while significantly outperforming agricultural residues such as rice husk (36–53 %) and cassava (37–42 %). Notably, it achieves this efficiency at lower pyrolysis temperatures than energy-intensive options like hazelnut shells (84.38 % at 1000 °C). Its balance of high carbon content, moderate processing temperature, and sustainable sourcing from invasive biomass positions P. Juliflora biochar as a competitive and eco-friendly material for cementitious composites, combining performance with circular economy advantages.

To evaluate the shape, size, and elemental composition of pyrolyzed particles, scanning electron microscopy (SEM) and energy dispersive X-ray spectroscopy (EDX) were performed. Spectrographs were obtained at various magnifications to accurately visualize the particle shape. For the EDX analysis, different spots on the sample were selected to assess the amount of carbon retained after pyrolysis. The characterization of pyrolyzed particles using SEM and EDX provided insights into their morphology and elemental composition, which is crucial for understanding their influence on the properties of the biochar-modified mortar mixes.

In this study, a low biochar dosage range (0–0.2 % by weight of cement) was deliberately selected to investigate its role as a nucleation agent aimed at refining the microstructure and accelerating early-age hydration. This minimal dosage range was chosen to avoid the confounding effects often associated with higher biochar contents—such as reduced workability, increased porosity, and agglomeration—that have been reported when biochar is used at levels up to 10 % for carbon

Fig. 3. Biochar preparation: (Left) Pyrolyzed biomass showing the raw material after thermal decomposition. (Right) Fine biochar obtained after grinding and sieving, ready for incorporation into the mortar mix.

Fig. 2. Pyrolysis process of P. Juliflora sample: The biomass is subjected to thermal decomposition in a tube furnace under controlled conditions to produce biochar.

Table 4
Carbon content of various biomass feedstocks at different pyrolysis temperatures.

Feedstock	Temperature (°C)	C(%)	Ref.
Conocarpus wastes	800	84.97	[44]
Rice husk	500	36.06	[21]
Waste hazelnut shell	1000	84.38	[45]
Wood chips	500	77.23	[46]
Rice husk	500	53.07	[46]
Olive stone	500	76.6	[46]
Waste peanut shell	500	56.65	[47]
Rice husk	500	41.01	[28]
Date palms	700	69.32	[48]
Mixed wood	500	87.13	[49]
Corncob	500–600	41.66	[50]
Cassava rhizome	500–600	37.60	[50]
Cassava stem	500–600	41.55	[50]
Bagasse fiber	500	86.07	[35]
Pine needles	700	85.91	[35]
Millet	550	84.08	[34]
Maize	500	86.89	[34]

sequestration or filler applications. Existing studies [51,52] indicate that trace additions (≤0.5 %) can significantly enhance hydration kinetics and early strength by offering effective nucleation sites. Therefore, this dosage window was considered appropriate for isolating and evaluating biochar's efficiency as a microstructural modifier, without interference from bulk physical or rheological effects. Moreover, such low dosages align well with practical considerations such as cost-effectiveness and material scalability. Although the broader environmental or thermal benefits associated with higher dosages fall outside the scope of this study, the selected range addresses a key research gap by identifying the lower threshold at which hydration enhancement becomes significant.

Consequently, a total of five types of mortar samples were cast, including one control sample and four with biochar additions ranging from 0.05 to 0.2 wt% of cement. The mortar specimens were designated as BC0, BC0.05, BC0.1, BC0.15, and BC0.2, reflecting biochar additions of 0 %, 0.05 %, 0.1 %, 0.15 %, and 0.2 %, respectively, by weight of cement. The cement-to-sand (C/S) ratio was kept constant at 1:2. The workability of the mixes was evaluated using the flow table test, ensuring compliance with the permissible limits outlined in ASTM C-1437 [53]. A water-to-cement ratio of 0.47 was maintained consistently across all samples. Additionally, 1 % superplasticizer by weight of cement was added to all mixes to maintain workability and dispersion. The mix compositions for the samples are shown in Table 5, while the cast samples and their curing process are depicted in Fig. 4 (on the left) and Fig. 4(on the right), respectively.

All mixing, casting, and testing procedures were conducted under controlled laboratory conditions at a temperature of 24 ± 2 °C and relative humidity of 35 ± 3 %. To ensure consistent hydration and minimize moisture loss, the mortar specimens were sealed in plastic wraps for the first 24 h, after which they were demolded and cured in a water tank maintained at room temperature until the designated testing age. This curing method was adopted to provide a saturated environment, ensuring uniform strength development and reproducibility.

Fig. 4. Processes involved: (Left) Sample casting process showing the filling of molds with mortar and preparation for initial setting. (Right) Sample curing process in a water bath maintained at 25 ± 1 °C to ensure proper hydration and strength development.

3. Methods

The bulk density of biochar was measured using the pycnometer method [54]. To determine the water absorption capacity of the biochar, the filter paper method was employed [55]. In this procedure, 3 g of biochar was added to 100 g of water, and the mixture was placed in a sealed container for 24 h, allowing the biochar to absorb the water. After the 24-h period, the mixture was transferred onto pre-wetted filter paper to allow the free water to drain. This process helped in determining the amount of water absorbed by the biochar, providing insights into its porosity and water retention properties.

The water absorption capacity of biochar (g/g) was measured using the following equation:

$$Water\ Absorption\ Capacity = \frac{Weight\ of\ Water\ Absorbed}{Weight\ of\ biochar} \quad (1)$$

Where Weight of Water Absorbed is the difference in weight between the initial and final water content after the biochar has absorbed the water, and Weight of Biochar is the initial weight of the biochar sample used in the experiment. This equation allows the calculation of the amount of water absorbed per gram of biochar, providing a measure of its water retention capacity.

To effectively disperse biochar in the mortar mix, a sonication process was employed. Initially, 80 % of the calculated amount of water was placed in a beaker along with the required quantity of biochar. This mixture was subjected to sonication in a sonication bath for 30 min to achieve uniform dispersion of biochar particles. The sonication process, as illustrated in Fig. 5, helps to break down agglomerates and improve the homogeneity of the biochar-water mixture.

After sonication, the dry components, including a measured quantity of cement and sand, were introduced into a Hobart mixer. The mixer was operated at a low speed for 60 s to ensure the preliminary blending of the dry materials. Subsequently, the sonicated biochar-water mixture was gradually added to the dry cement-sand blend while the mixer continued to operate for an additional 90 s. To ensure thorough mixing, the mixer was stopped, and the mortar adhering to the sides of the bowl was scraped down into the mixture. Following this, the remaining 20 % of water and 1 % high-range water-reducing admixture (HRWRA) were introduced into the mix. The mixer was then operated at high speed for

Table 5
Mix design and composition of mortar samples with varying biochar percentages.

Sr. No	Sample	C/S Ratio	W/C	Biochar age)	Cement (gm)	Sand (gm)	Water (gm)	HRWRA (gm)
1	BC0	1:2	0.47	0 %	530	1060	243.8	5.3
2	BC0.05	1:2	0.47	0.05 %	530	1060	243.8	5.3
3	BC0.1	1:2	0.47	0.10 %	530	1060	243.8	5.3
4	BC0.15	1:2	0.47	0.15 %	530	1060	243.8	5.3
5	BC0.2	1:2	0.47	0.20 %	530	1060	243.8	5.3

Fig. 5. Sonication process of biochar: Ultrasonic waves are applied for 30 min to disperse biochar uniformly in 80 % of the calculated water, ensuring effective integration into the mortar mix.

150 s to achieve a uniform and workable mortar mix.

The prepared mortar was then transferred into moulds of two types: prism moulds measuring 40 × 40 × 160 mm and cube moulds measuring 50 × 50 × 50 mm. The moulds were carefully filled and compacted to minimize air voids. To prevent moisture loss during the initial setting period, the moulds were covered with polythene sheets and left undisturbed at room temperature for 24 h. After 24 h, the hardened samples were demoulded and transferred to a water bath maintained at 25 ± 1 °C for curing. The curing process ensures adequate hydration, improving the strength and durability of the mortar samples. Once, the specimens have been matured, they were tested for various properties at different ages.

Flexural strength was evaluated using the ASTM C348 method [56], which involves applying a central load to prism specimens until failure to measure their resistance to bending. The testing setup is illustrated in Fig. 6(left). Following the flexural strength test, the fractured halves of the prisms were repurposed for compressive strength testing. This test, conducted in accordance with ASTM C349 method [57], determines the compressive strength of the material by applying a compressive load to the broken prism halves. The setup for the compressive strength test is depicted in Fig. 6(right).

The procedure for measuring porosity was as follows [58]: The specimen was removed from the curing tank and its surface was gently wiped to remove any excess moisture. The initial weight of the sample (Ms) was recorded. The sample was then placed in an oven at 105 °C for 24 h. After the drying period, the weight of the sample (MOD) was measured again. Porosity is calculated as the ratio of weight loss to the initial dry mass (Mi) of the sample, where Mi is the mass measured after 24 h of casting and before immersion in water for curing.

The porosity is expressed by the Eq. (2):

$$P\ (\%) = \frac{(Ms - MOD)}{M_i} \cdot 100 \quad (2)$$

The carbonation test was conducted in accordance with RILEM CPC-18 [59] and BS EN 14630:2006 [60] standard methods . The cubical sections (50×50×50 mm) from each type of samples (BC0, BC0.05, BC0.1, BC0.15 and BC0.2) were taken out from the curing tank after curing for 28 days. These samples were exposed to the natural atmosphere sheltered from rain for a period of 24 months. Measurements were taken after 24 months of natural exposure. The samples were cut through the middle with the help of a cutter. The freshly cut surface was cleaned with brush and was sprayed with fine mist of phenolphthalein 1 % solution. Phenolphthalein is commonly used as a pH indicator. It becomes pink in basic solutions and shows no color in acidic solutions. This method is used to detect concrete surfaces which are completely carbonated, moderately carbonated or not carbonated at all. After spraying the surfaces were observed for carbonation. In case of weak coloration, the samples were sprayed again after half an hour.

The ASTM C666 / C666M method [61] was used to determine the freeze and thaw resistance of the specimens. The cube specimens 50×50×50 mm were removed from the curing tank after 56 days and oven-dried at 105 °C until a constant mass was achieved. The dried samples were then re-saturated in water for seven days. After surface moisture was removed, freeze-thaw testing was carried out in two steps: Step 1—specimens were frozen in air at –20 to –18 °C for 6 h; Step 2—they were thawed in water at 18 to 20 °C for another 6 h. Mass loss and compressive strength were evaluated after 100 freeze-thaw cycles.

For determining the resistance to heat, control and biochar mortar specimens were cured for 90 days, air-dried, then oven-dried at 105 °C for 24 h. After cooling, samples were heated in a furnace from 20 °C to 450 °C at 5 °C/min and held at 450 °C for 45 min. They were cooled inside the furnace for one day to avoid thermal shock [62]. Post-heating, mass loss, compressive, and flexural strengths were evaluated in accordance with the relevant ASTM methods.

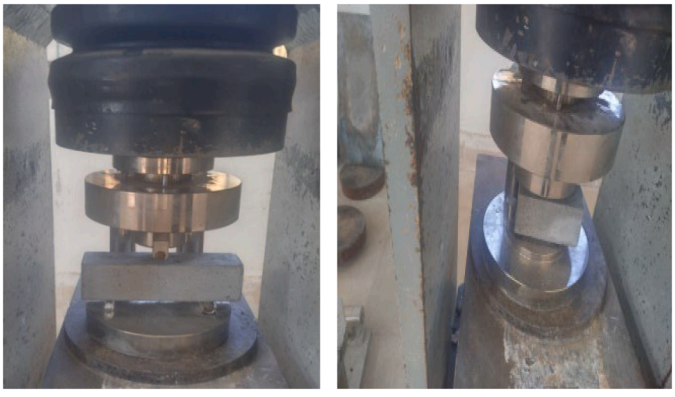

Fig. 6. Testing setups: (Left) Flexural strength test conducted as per ASTM C348 to measure the resistance of prism specimens to bending. (Right) Compressive strength test performed on broken halves of prisms following ASTM C349 to evaluate compressive strength.

4. Results and discussion

4.1. Biochar

4.1.1. Bulk density

The bulk density of biochar was found to be 0.3 g/cm^3, which is significantly lower than that of common construction materials such as cement (3.15 g/cm^3) and sand (1.5 g/cm^3). This lower bulk density can be attributed to the porous and lightweight nature of biochar [9,63]. Such a structure includes a network of micro- and mesopores that reduce particle mass while increasing surface area. As a result, when incorporated into cementitious matrices, biochar can influence the composite's density, reduce overall weight, and potentially improve thermal insulation [64,65]. Comparable trends have been reported in previous studies utilizing biochar from other biomass sources, such as wood and rice husk, which demonstrated similar reductions in composite density and enhanced sustainability benefits [30,66]. Hence, the low bulk density of P. Juliflora biochar not only reflects its physical nature but also supports its suitability for lightweight mortar applications.

4.1.2. Water absorption

The water absorption capacity of P. Juliflora biochar was measured at 2.83 g/g, indicating that each gram of biochar can absorb up to 2.83 g of water. This elevated capacity is attributed to its highly porous structure, which comprises both micropores and macropores formed during pyrolysis [67]. The result aligns with the previously observed low

bulk density, as both properties stem from the same cellular architecture of biochar. High water absorption in biochar can play a significant role in cementitious composites. Specifically, biochar can function as an internal curing agent by gradually releasing absorbed water during the hydration process [68,69]. This mechanism may enhance the degree of hydration, reduce autogenous shrinkage, and mitigate early-age cracking—especially in hot or dry curing environments [70]. These benefits have been reported in literature using biochars derived from other biomass sources such as rice husk and wood, which similarly exhibited internal curing effects and improved mechanical performance [30,66]. Therefore, the water absorption capacity of P. Juliflora biochar is not only indicative of its porous microstructure but also highlights its functional potential in enhancing concrete performance through internal moisture regulation.

4.1.3. Scanning electron microscopy

SEM images of biochar are shown in Fig. 7a, Fig. 7b, and Fig. 7c. The particle size ranges from nanoscale to microscale, as seen in Fig. 7a. The texture of the particles is rough, with visible ridges on their surfaces, as highlighted in Fig. 7b. The pores formed in the structure due to the release of volatile components during biomass pyrolysis are evident in Fig. 7c. The porous and rough texture of biochar contributes to the enhancement of the strength and ductility of cement composites [71]. These physical characteristics provide a greater surface area and mechanical interlocking at the biochar–cement paste interface, promoting better adhesion between the particles and the cementitious matrix [72]. The rough texture facilitates mechanical anchorage, which contributes to an improved load-transfer mechanism within the composite and reduces the likelihood of interfacial failure [73]. The rough biochar particles act as crack-arresters, deflecting and bridging microcracks during loading, which improves the post-peak ductility and energy absorption capacity of the composite [74]. Several studies have reported improved mechanical properties—including splitting tensile strength, flexural strength, and toughness—when biochar with high surface roughness and porosity is used in cementitious materials [63,75]. Therefore, the unique surface morphology of biochar derived from P. Juliflora is not merely a physical attribute, but a functional advantage in tailoring the mechanical performance of sustainable cement composites.

4.1.4. Energy-dispersive X-ray spectroscopy

An Energy-dispersive X-ray spectroscopy (EDX) analysis was conducted, and the results are presented in Table 6. The biochar exhibited a high Carbon content of 83.09 %, indicating that the pyrolysis process effectively retained Carbon in the biochar. This retention prevents the release of Carbon into the atmosphere as CO_2, which would otherwise occur through the burning or decomposition of biomass.

When compared with other biomass-derived biochars listed in Table 4, this value is among the highest reported. For instance, it is comparable to that of Conocarpus waste (84.97 %), bagasse fiber (86.07 %), maize (86.89 %), and pine needles (85.91 %), all of which were processed at relatively high pyrolysis temperatures (typically ≥700 °C). Conversely, biomass sources like rice husk (ranging from 36.06 % to 53.07 %) and cassava rhizome (37.60 %) showed significantly lower carbon content even at similar or slightly elevated temperatures. Given that P. Juliflora is an invasive species in many arid regions, converting it into high-carbon biochar provides an ecologically responsible disposal route while enhancing sustainability in construction.

Table 6
Elemental composition of P. Juliflora biochar based on EDX analysis.

Analysis	Carbon	Oxygen	Magnesium	Potassium	Calcium
Composition (%)	83.09	12.59	0.09	1.72	0.2

4.2. Biochar added mortar

4.2.1. Effect of admixture on flow

The effect of admixture on flow is indicated by Figs. 8 and 9. In Fig. 8, the mortar specimens before the flow table test are shown. Whereas in Fig. 9, the effect of admixture on flow is presented.

It is evident that the addition of biochar influences the flowability of the mortar. In Fig. 9(c), where 0.2 wt% biochar is added without any admixture, the flow is reduced despite improved biochar dispersion. This is primarily due to the water absorption capacity of biochar, which decreases the amount of free water available for lubrication. As a result, the mix appears fractioned and less cohesive. In contrast, Fig. 9(d), which includes both biochar and a water-reducing admixture, exhibits significantly improved flow. The admixture compensates for the absorbed water, restoring lubrication and enhancing overall workability.

4.3. Porosity

The porosity data are presented in Fig. 10. During the curing period, prolonged immersion in water ensures complete saturation of the pores in the sample. Therefore, porosity was determined by measuring the loss of water mass during oven drying, which corresponds to the volume of pores initially filled with water.

The porosity appears to decrease initially with increasing biochar content, reaching a minimum at a dosage of 0.1 %. However, beyond this percentage, the porosity slightly increases again. The initial decrease in porosity could be attributed to the biochar particles filling the voids in the matrix, thereby reducing the total pore volume, as also noted. Previous studies have shown that moderate incorporation of biochar can improve the pore structure of cementitious composites by

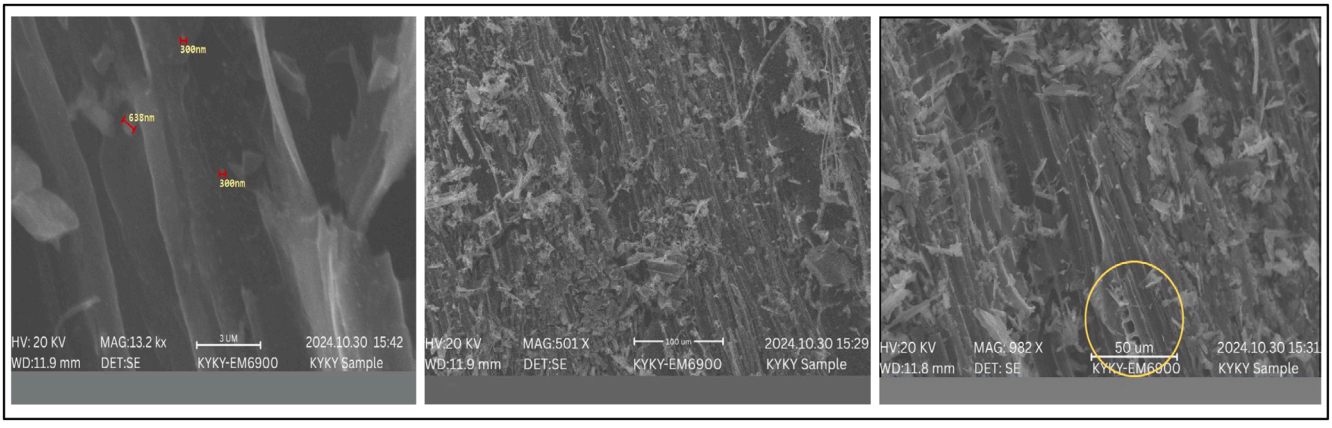

Fig. 7. SEM images of biochar: (a) Particle size ranging from nano to micrometers, (b) Ridges and rough surface texture, (c) Capillary pores formed due to volatile component release during pyrolysis. The porous and rough texture of biochar is beneficial for enhancing the strength and ductility of cement composites.

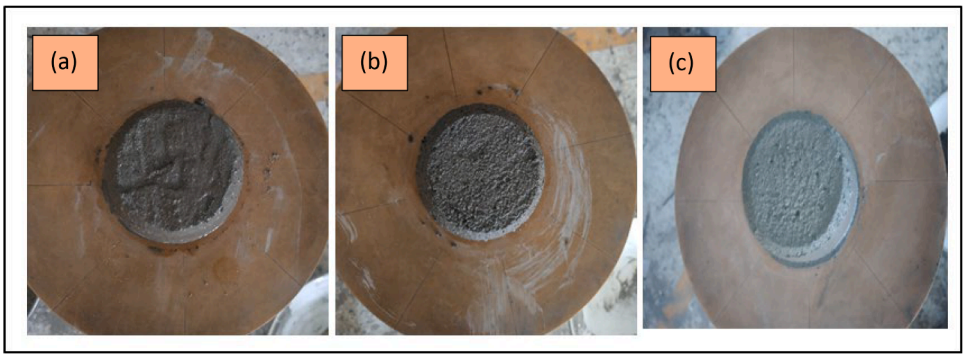

Fig. 8. (a) shows that the specimen has visible surface water, indicating excess free water in the mix. Upon the addition of 0.2 % biochar, as seen in Fig. 8(b), the free water disappears and the surface appears relatively drier, suggesting that biochar particles absorb part of the free water due to their porous structure. In contrast, Fig. 8(c) illustrates that with the addition of a chemical admixture, the specimen becomes noticeably more flowable, likely due to improved dispersion and reduced inter-particle friction.

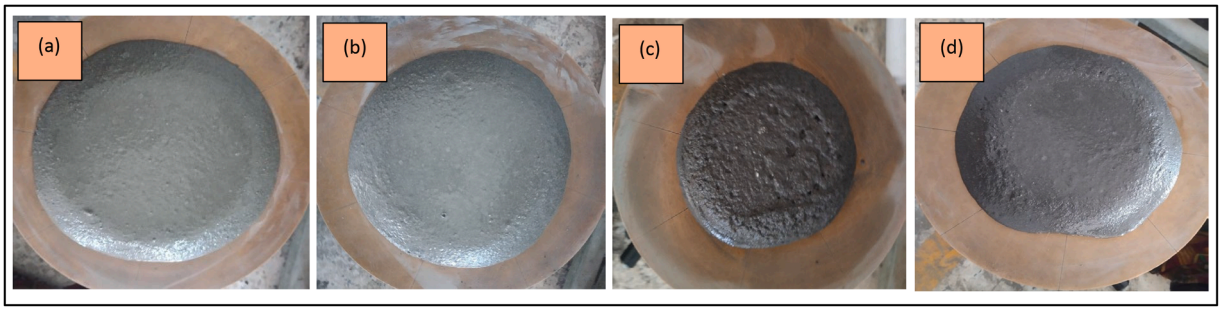

Fig. 9. Final flow diameters of mortar specimens (left to right): (a) 1 wt% water-reducer (W.R) without biochar, (b) 0.1 wt% biochar with 1 wt% W.R, (c) 0.2 wt% biochar without W.R, and (d) 0.2 wt% biochar with 1 wt% W.R.

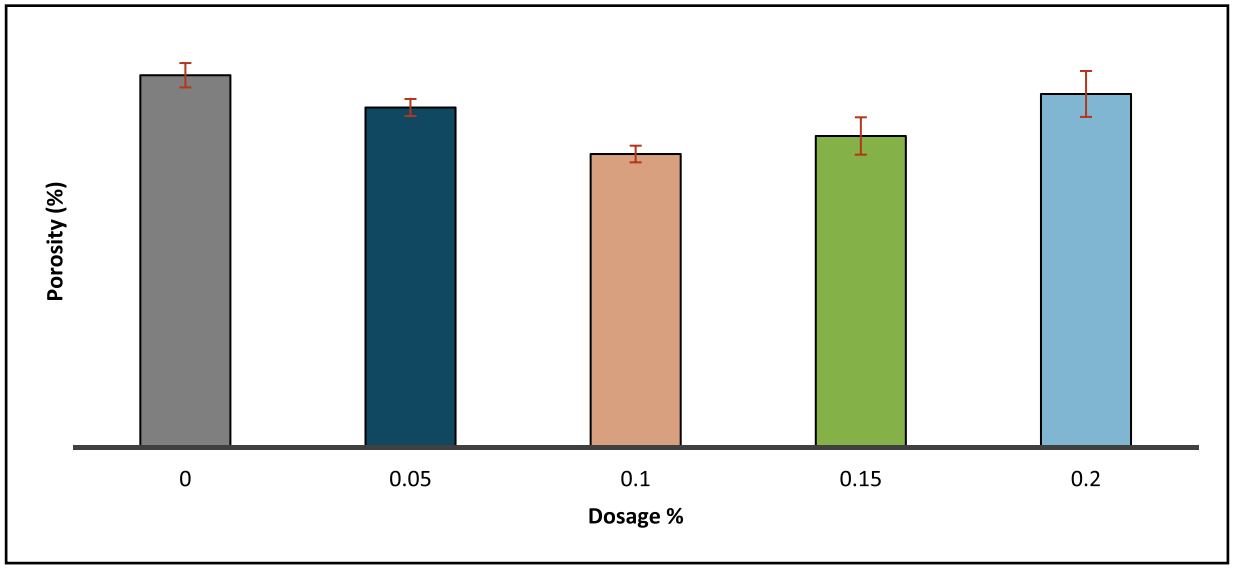

Fig. 10. Variation of porosity with increasing biochar content from Prosopis Juliflora. The initial decrease in porosity indicates a densification effect at lower biochar dosages due to water absorption by biochar, reducing free water available for capillary porosity. The subsequent increase in porosity at higher dosages is attributed to the low density and porous nature of biochar, as well as potential particle aggregation.

filling voids and refining the microstructure [28,51]. However, as the dosage increases beyond an optimal threshold (e.g., 0.1 % in this study), porosity tends to rise again. This increase is likely due to the agglomeration of biochar particles, which disrupts the homogeneity of the mix and introduces interconnected voids or microcracks during curing [21,76]. Additionally, biochar's intrinsically porous nature contributes to the overall pore volume when used in excess, potentially offsetting the initial densifying effect [76]. High dosages may also increase the water demand of the mix and interfere with normal hydration kinetics, leading to incomplete matrix formation and a less compact microstructure [77,78]. This trend underscores the importance of optimizing biochar dosage to balance its beneficial effects on internal curing and

microstructure densification with the potential drawbacks associated with excessive incorporation.

The standard deviation in porosity varies across the dosages, with the lowest variability observed at 0.1 %, indicating highly consistent results. In contrast, the highest variability appears at 0.2 %, while the control and intermediate dosages show moderate fluctuations. This increased variability at higher dosage may be attributed to factors such as poor dispersion, agglomeration, or disturbance in the matrix homogeneity. Overall, the results suggest that lower dosages lead to more stable and predictable porosity outcomes, while higher dosages introduce greater uncertainty in the microstructure. The coefficients of variations vary from 3 to 6 % from BC0 to BC0.2, all are lower than 10 %. This indicates a generally low level of variability in the porosity measurements [79].

4.4. Hardened density

The 90-day hardened density of the mortar specimens is shown in Fig. 11. The addition of biochar increased the density of the specimens, with the average maximum density (2.09 g/cm^3) observed at 0.1 wt% biochar. Beyond this dosage, the density decreases but remains higher than that of the control specimen.

This initial densification is attributed to the water absorption capability of biochar, which reduces the amount of free water in the mix, thereby limiting capillary porosity and contributing to a more compact microstructure [28]. Additionally, the fine biochar particles can occupy micro voids within the matrix, further enhancing packing density. However, beyond the optimal 0.1 wt% dosage, the density begins to decline. This is likely due to the intrinsically low bulk density and porous structure of biochar, which becomes more influential at higher dosages, reducing the overall mass per unit volume of the composite [80]. The tendency of biochar to agglomerate at elevated concentrations may also disrupt homogeneity, leading to localized voids and incomplete consolidation [35,81]. These findings closely mirror the trends observed in the porosity analysis—where a reduction in porosity at low biochar content aligns with increased density, and a rise in porosity at higher content correlates with decreased density. This inverse relationship between porosity and density highlights the dual role of biochar in modifying mortar structure and underscores the importance of dosage optimization to balance its beneficial effects on microstructural densification against potential drawbacks at higher inclusion levels.

The results consistently show small error bars, suggesting low variability in the results. Across all dosages from 0 % to 0.2 %, the error bars indicate that the density values are tightly clustered around the mean. This consistent pattern suggests that the experimental conditions and material behavior remained stable, regardless of dosage level. The coefficients of variation vary from 2 % to 5 %, indicating a low level of variability and stable behavior across all dosages.

4.5. Compressive strength

Compressive strength development of mortar samples containing biochar, alongside control samples, is presented for 3, 7, 28, and 90 days in Fig. 12. The inclusion of biochar consistently enhanced the compressive strength compared to the control mortar across all time intervals. At 3 days, the highest compressive strength (34.7 MPa) was observed in the sample with 0.1 wt% biochar, compared to 32.8 MPa in the control. At 7 days, the maximum strength increased further, reaching 39.3 MPa for the 0.1 wt% biochar sample, compared to the control strength of 35.2 %. At 28 days, the trend continued, with the 0.1 wt% biochar sample achieving a maximum compressive strength of 64.4 MPa, higher than that of the control with 57.84 MPa. At 90 days, the peak strength of 68.97 MPa was noted for the 0.1 wt% biochar sample with 61.84 MPa for the control specimen.

In all cases, the compressive strength decreased at higher biochar dosages but remained above the control values, demonstrating that biochar addition—particularly at an optimized dosage of 0.1 wt% effectively enhances the compressive strength of mortar.

The strength enhancement at low dosages can be attributed to the unique morphology and intrinsic properties of biochar. As shown in Fig. 7b, biochar particles possess a rough and elongated surface, which facilitates mechanical interlocking and improved bonding with the cement matrix [51]. Moreover, biochar's porous structure and high surface area enable it to absorb and retain mixing water [82–84]. This absorbed water is gradually released due to moisture gradients, aiding internal curing and promoting continued hydration [36,85]. According to Gray et al. [86], biochar derived from high-carbon feedstocks exhibits enhanced water absorption capabilities, contributing to matrix densification by reducing pore volume. These mechanisms are further

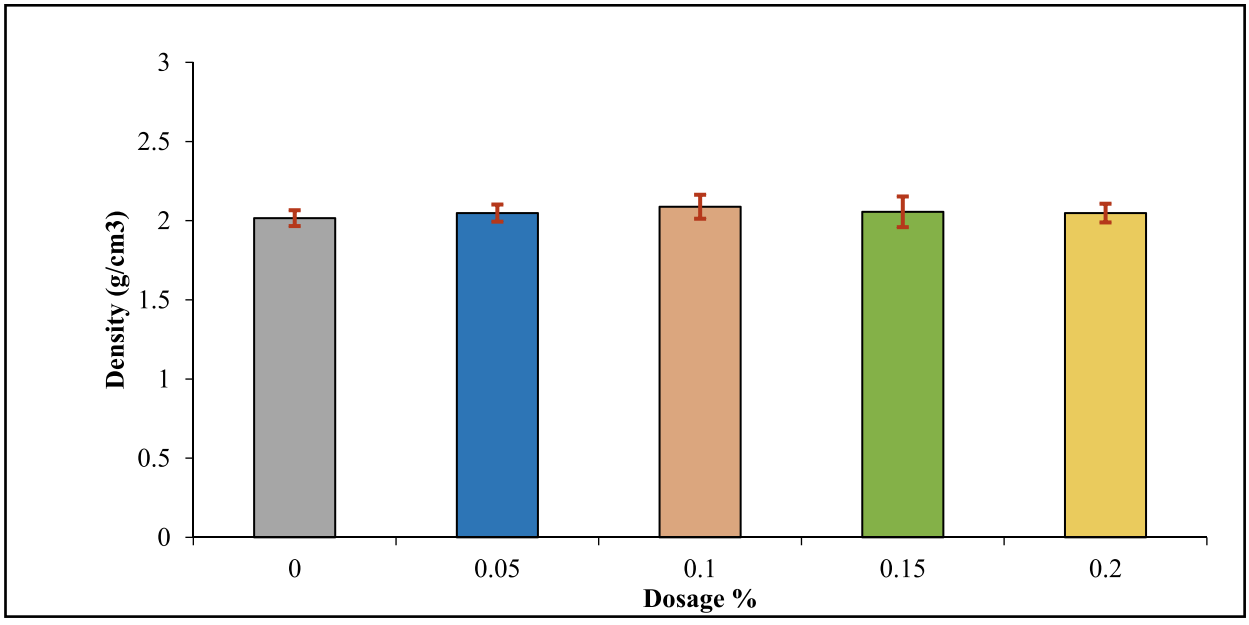

Fig. 11. 90-day hardened density of mortar specimens with varying biochar content from Prosopis Juliflora. The maximum density (2.09 g/cm^3) is observed at 0.1 wt% biochar addition, attributed to the densification effect caused by water absorption at low dosages. At higher dosages, density decreases due to the porous and lightweight nature of biochar, yet it remains higher than the control specimen.

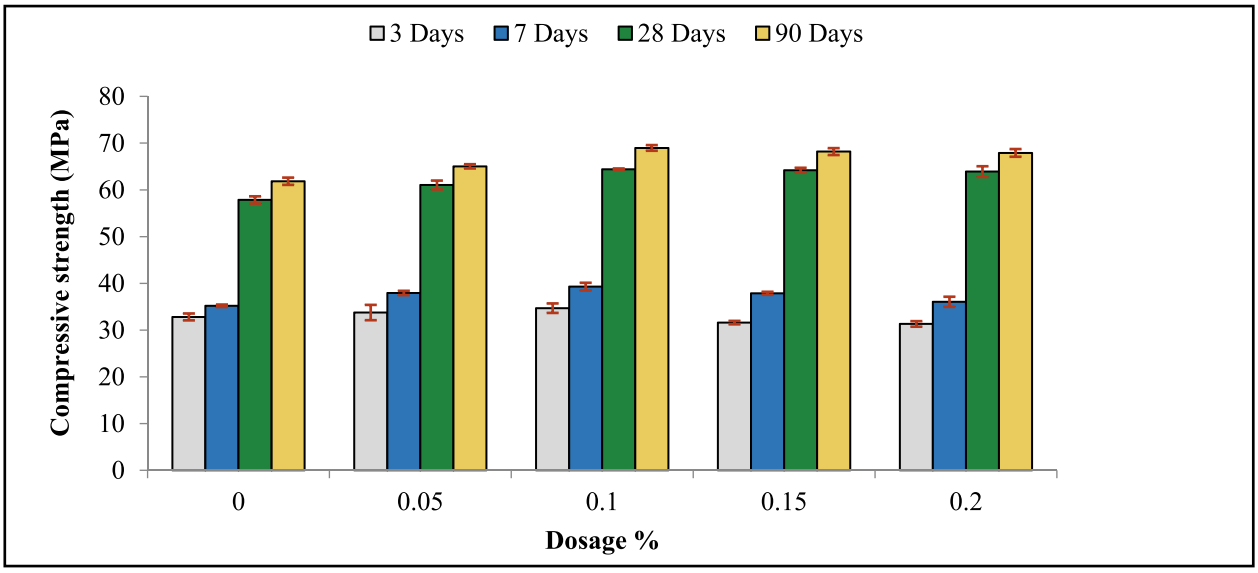

Fig. 12. Compressive strength (measured in MPa) of cement sand mortar at four curing periods (3, 7, 28, and 90 days) across different dosages of P. Juliflora biochar (0 %, 0.05 %, 0.1 %, 0.15 %, and 0.2 %). The maximum compressive strength (69 MPa) is observed at 0.1 wt% biochar addition, attributed to the highest density and the lowest porosity at this dosage.

supported by the presence of capillary pores visible in Fig. 7c.

However, beyond 0.1 wt%, the compressive strength declined slightly, though it remained higher than the control. This reduction is likely due to the increased porosity and low bulk density of excess biochar, which compromises matrix integrity. Similar findings have been reported in literature. Sirico et al. [6] found peak strength at 1 wt% wood-chip biochar, while Jiang et al. [85] observed optimal performance at 1 wt% wheat/rice straw biochar. Navaratnam et al. [62] also reported maximum strength at 0.5 wt% addition. Ahmad et al. [83] documented strength improvement up to 0.08 % bamboo biochar, beyond which strength diminished. These studies consistently highlight an optimal biochar dosage—typically between 0.05 and 1 wt%—beyond which negative effects such as poor packing and increased porosity dominate.

Gupta et al. [30] further demonstrated that excessive addition (beyond 2 wt%) of low-temperature wood biochar reduced strength due to the light and porous nature of biochar. Goldman and Bentur [87] explained that strength enhancement is primarily due to the filler effect of biochar particles and their ability to absorb free water, effectively reducing the water-to-cement ratio and thus limiting capillary porosity. This aligns with the observed strength gains in this study, reinforcing that 0.1 wt% biochar addition is optimal for compressive strength enhancement.

The compressive strength results show consistently short error bars across all ages and dosages, indicating low variability. With coefficients of variation ranging from < 1 % to 5 %, the data reflects stable, reliable, and reproducible strength development over time.

4.6. *Relationship between strength, density, and porosity*

The relationship between compressive strength and density is shown in Fig. 13, where a clear correlation is observed. Density increases with biochar content up to 0.1 wt% of cement and then decreases. Similarly, compressive strength follows the same trend, increasing up to 0.1 wt% biochar content before declining.

Fig. 14 highlights the inverse relationship between porosity and compressive strength in the biochar-modified mortar samples. Up to an optimal dosage of 0.1 wt% biochar, porosity decreases, resulting in a

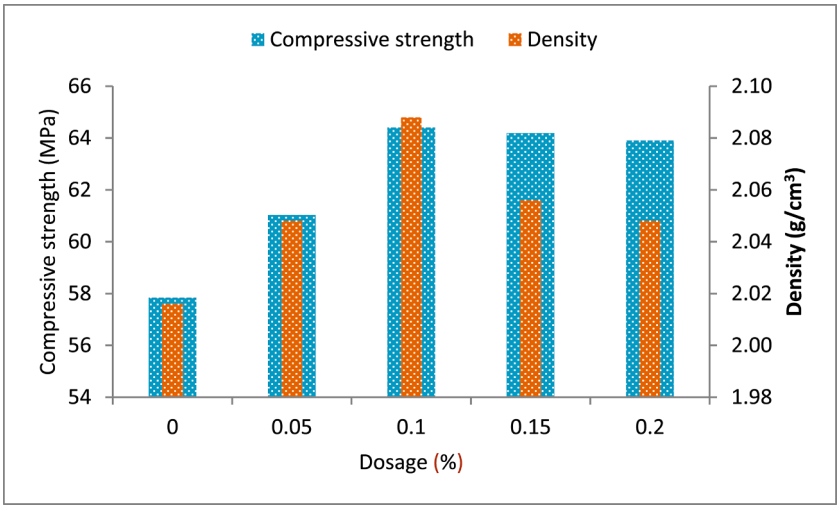

Fig. 13. Correlation between biochar dosage, density, and compressive strength of cement-sand mortar prepared with P. Juliflora biochar. The graph highlights the peak density and compressive strength at a 0.1 % biochar dosage, followed by a gradual decline as biochar content increases.

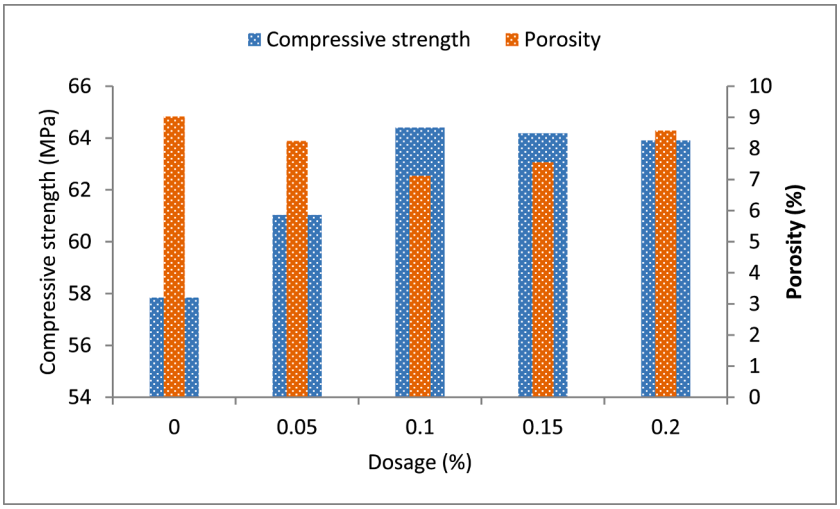

Fig. 14. Relationship between porosity and compressive strength of cement-sand mortar incorporating P. juliflora biochar at varying dosages. The figure highlights the optimal dosage at 0.1 %, where compressive strength reaches its maximum and porosity its minimum. Beyond this point, strength decreases, and porosity increases.

corresponding increase in compressive strength. This densification of the matrix can be attributed to three primary mechanisms: (i) the filling of nano- and micropores by biochar particles, (ii) the reduction of capillary pores due to biochar's ability to absorb and retain mixing water, and (iii) the facilitation of internal curing, whereby the stored water is gradually released during hydration. These mechanisms collectively contribute to enhanced hydration kinetics and matrix compaction, thereby improving mechanical performance.

Beyond 0.1 wt%, porosity increases with additional biochar content, leading to a decline in compressive strength. This can be explained by the introduction of excessive voids and discontinuities within the matrix due to the inherently low density and high porosity of surplus biochar. Similar observations have been reported in the literature, where over-dosage of biochar compromises the packing density and disrupts matrix continuity. The internal curing effect observed in this study is further supported by the work of Choi et al. [29], who demonstrated that water physically bound within the porous structure of biochar is gradually released, promoting sustained hydration and improved strength development.

4.7. Flexural strength

The flexural strength test results are presented in Fig. 15. The data indicate that the addition of biochar enhances the flexural strength of mortar compared to the control. Flexural strength increases with biochar content up to 0.1 wt% of cement, after which it begins to decrease. At 28 days of curing, a 0.1 wt% addition of biochar results in a 17 % increase in flexural strength, while at 90 days, the increase reaches 21 %. Although the flexural strength declines with biochar content beyond 0.1 wt%, the values remain higher than those of the control mortar at 7, 28, and 90 days.

Biochar particles enhance the flexural strength of the mortar matrix through two primary mechanisms. First, they provide nucleation sites for the deposition of calcium hydrate products, resulting in a stronger matrix [49]. The second and more dominant factor is the alteration of the crack propagation path with the addition of biochar. In a pure cement matrix, cracks propagate rapidly once they are initiated, leading to sudden specimen failure. In contrast, in a biochar-mortar composite, growing cracks are trapped and diverted, creating a longer propagation

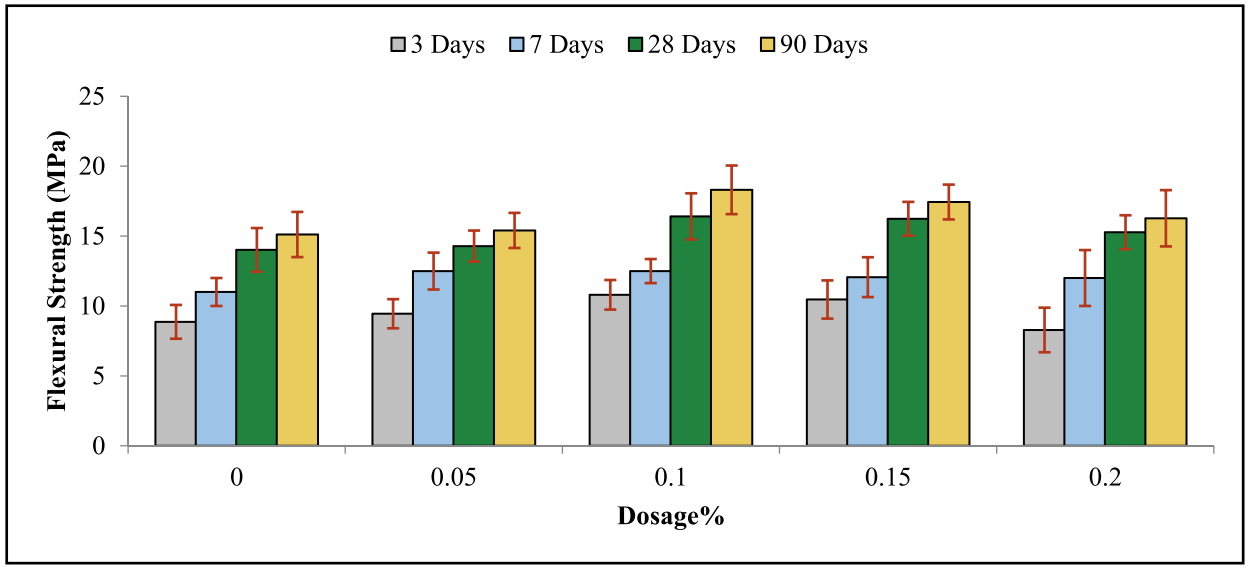

Fig. 15. This graph shows the flexural strength (MPa) of specimens with varying biochar dosages (0 % to 0.2 % wt.) of P. Juliflora over 3, 7, 28, and 90 days. Flexural strength increases with biochar, peaking at 0.1 % wt. before decreasing at higher dosages, with all values surpassing those of the control specimens.

route. This delayed crack progression allows the sample to bear additional load, thereby increasing its flexural strength [83].

Contrary to the previous results, higher variability was observed in flexural strength results. The coefficients of variation ranged up to 20 %. This can be attributed to the greater sensitivity of flexural strength to microstructural flaws and testing conditions [88]. Flexural strength is more influenced by surface defects, voids, and microcracks, which may arise due to the heterogeneous nature of biochar and its uneven dispersion within the matrix. Unlike compressive strength, which reflects bulk material behavior, flexural strength is governed by tensile stresses and is highly dependent on the quality of the matrix-particle interface. Any inconsistencies in bonding or particle distribution can initiate cracks under bending loads, increasing result variability. Moreover, flexural testing methods, involving smaller and more slender specimens, are more susceptible to alignment errors, surface imperfections, and loading inconsistencies [56]. These factors may contribute to the higher variability in flexural strength compared to the relatively stable and reproducible results seen in density, porosity, and compressive strength.

Fig. 16 demonstrates the influence of biochar on crack propagation and flexural strength in cement mortar. With the inclusion of biochar, visible branching and discontinuities appear along the crack paths, indicating a transition from singular to more tortuous crack trajectories. This behavior is attributed to the inert, carbon-rich nature of biochar, which, while acting as a heterogeneity in the matrix, resists degradation and deflects cracks rather than allowing their direct propagation [84]. The altered crack morphology suggests that biochar contributes to energy dissipation during fracture, thereby enhancing the composite's resistance to crack growth.

The biochar used in this study exhibited rough, angular, and fibrillar morphology (Fig. 7), allowing it to function as both a micro-filler and a reinforcing phase. This morphology promotes mechanical interlocking within the matrix and enhances the interfacial bond. Restuccia and Ferro [89] similarly observed that jagged biochar particles integrate effectively within the cementitious matrix, altering the fracture mechanism. This interfacial behavior is particularly relevant in the interfacial transition zone (ITZ), which typically spans 10–40 μm in plain mortars [90] and plays a critical role in defining mechanical performance.

Flexural strength results (Fig. 15) show an enhancement with the biochar addition up to 0.1 wt%, beyond which the strength declines. The initial improvement is likely to be due to improved matrix integrity, crack deflection, and better stress transfer facilitated by well-dispersed biochar particles. The results are consistent with Khushnood et al. [91], who reported a 42 % increase in flexural strength with biochar derived from hazelnut shells. However, feedstock variability significantly affects performance; for example, Ahmad et al. [82] noted a reduction in flexural strength with coconut shell biochar. These disparities emphasize that not only the dosage but also the physicochemical properties of the biochar (influenced by feedstock and pyrolysis conditions) are critical.

At dosages beyond 0.1 wt%, the flexural strength decreases, consistent with findings by Gupta et al. [28], who attributed this to increased porosity and matrix inhomogeneity. Excessive biochar tends to entrap air and disrupts the continuity of the cement matrix, reducing the effective bonding area and weakening the mortar under bending stresses. Similar observations have been reported in the literature for other additives, such as pottery and brick powder, supporting the notion that excessive inclusion can compromise matrix integrity [92]. Therefore, optimizing both dosage and biochar characteristics is essential to harness its reinforcing potential without compromising the structural integrity.

4.8. Resistance to carbonation

Concrete structures are constantly exposed to CO_2, leading to carbonation, which reduces durability and service life. Carbonation occurs in four steps: (1) CO_2 forms carbonic acid in moisture, (2) it reacts with $Ca(OH)_2$ and C-S-H, reducing strength, (3) insoluble $CaCO_3$ converts to a soluble phase, and (4) Calcium is dissolved leaving porous silica gel [93]. This process lowers pH, causing steel reinforcement corrosion, further compromising concrete integrity [94]. The carbonation results are shown in Fig. 17. The results indicate that the control sample experienced the most carbonation, while biochar-containing samples showed reduced carbonation, with the least carbonation at 0.1 wt% biochar. Carbonation depth decreased to 0.15 wt% biochar and then increased to 0.2 wt%, though it remained lower than the control.

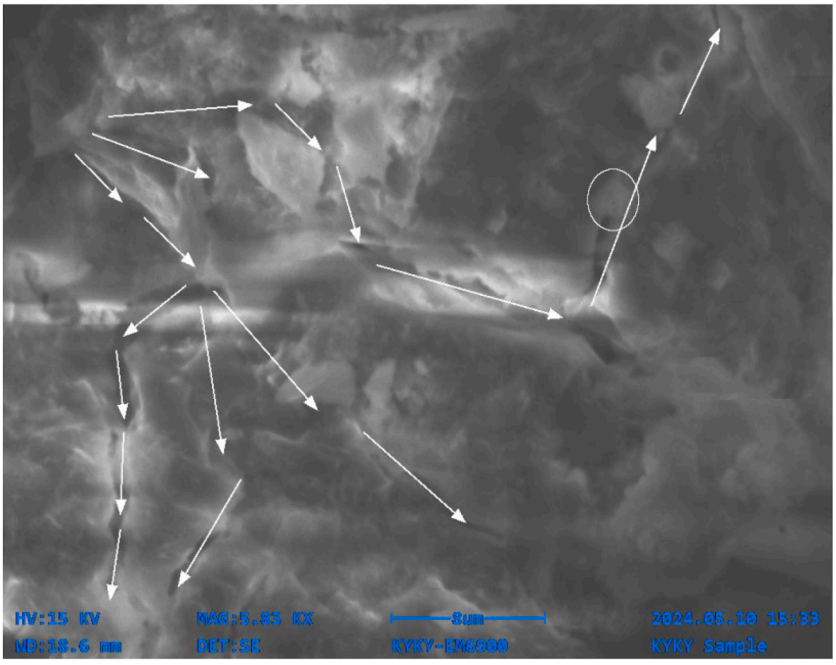

Fig. 16. This image illustrates the crack diversion and increased tortuosity in cement sand mortar with the addition of P. Joliflora biochar. The biochar particles enhance the mortar's resistance to crack propagation, leading to a more tortuous crack path and improved durability.

Fig. 17. This image shows five concrete specimens after the phenolphthalein carbonation test, arranged from right to left in order of increasing biochar content (0, 0.05, 0.1, 0.15, and 0.2 wt%). Pink regions indicate uncarbonated areas (high pH), while colorless areas represent carbonated zones (low pH due to CO_2 reaction).

Studies suggest that biochar improves hydration, densifies the cement matrix, and reduces porosity, contributing to lower carbonation [26,29,95]. XRD analysis (Fig. 18) confirmed biochar's inert nature but showed reduced calcium carbonate peak intensity, indicating slower carbonation. The reduction in carbonation correlates with increased density and reduced porosity, both optimized at 0.1 wt% biochar.

Visual evidence in Fig. 17 reinforces these findings, where the specimens are arranged from right to left in order of increasing biochar content (control → 0.05 wt% → 0.1 wt% → 0.15 wt% → 0.2 wt%). The control sample (rightmost) displays the most extensive carbonation, visible as a broader uncoloured region caused by the reaction between phenolphthalein and CO_2. In contrast, the 0.1 wt% biochar specimen shows the smallest carbonation zone, indicating the highest resistance to CO_2 diffusion. Slight increases in carbonation depth beyond 0.1 wt% suggest that excessive biochar content may reintroduce microstructural voids due to its inherently porous nature, slightly offsetting the densification benefit. Complementing the physical test, the XRD analysis (Fig. 18) supports these trends. While the biochar itself is inert—as indicated by the absence of new crystalline phases—reduced peak intensities of calcium carbonate in the biochar-containing sample (particularly at 0.2 wt% of P. juliflora biochar) point toward slower carbonation kinetics. This further validates the inference that biochar modifies the matrix in a way that impedes carbonation progression.

Overall, the results confirm that 0.1 wt% biochar is the optimal dosage for minimizing carbonation in cement mortar. Beyond this threshold, the increase in porosity may outweigh the benefits of internal curing and densification, resulting in slightly diminished performance.

The XRD patterns (Fig. 18) compare the control (black) and biochar-modified (red, 0.2 wt% P. Juliflora biochar) mortar samples after carbonation. The control sample shows a stronger $CaCO_3$ (C) peak, indicating higher carbonation, while the biochar sample retains more Ca $(OH)_2$ (E peak), suggesting delayed carbonation due to enhanced hydration and matrix densification [96]. The AFm phases (D peaks) remain stable in the biochar sample, indicating minimal disruption to cement hydration [97]. Additionally, SiO_2 (A) and C_2S (B) peaks appear in both samples, confirming that biochar does not alter the primary silicate phases. These findings suggest that biochar improves carbonation resistance by enhancing the internal curing effect and reducing CO_2 penetration [98]. Previous studies have shown that P. juliflora biochar exhibits a mesoporous microstructure, with a specific surface area of 72 m^2/g and a pore volume of 0.083 cm^3/g, which supports internal curing and promotes matrix densification [99]. Furthermore, X-ray Photoelectron Spectroscopy (XPS) analysis by Daud et al. (2021) revealed a high concentration of surface oxygen-containing functional groups in biochar of P. juliflora [100]. These functionalities, more abundant than those typically found in wood- or rice-husk-derived biochars, enhance water adsorption and provide effective nucleation sites for cement hydration products.

4.9. Freeze and thaw resistance

The freeze and thaw resistance were checked through three ways: (1) surface changes, (2) mass loss, and (3) residual compressive strengths. The surface changes that occurred after 100 cycles are shown in Fig. 19.

The control specimen (0 % biochar) exhibits significant surface deterioration, microcracking, and scaling, indicating poor freeze-thaw resistance. With 0.05 % biochar, surface damage is slightly reduced, while 0.1 % biochar shows minimal deterioration, suggesting enhanced resistance due to internal curing effects. Internal curing enhances freeze-

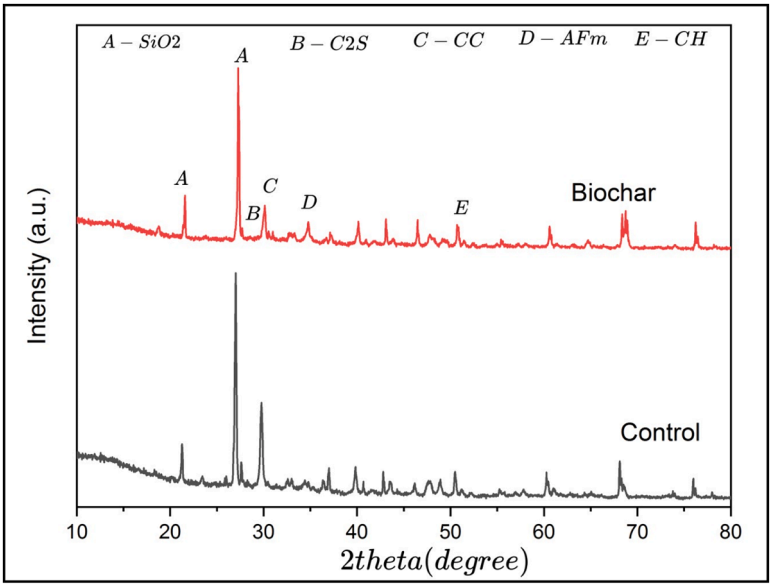

Fig. 18. XRD Patterns of Control and Biochar-Modified Mortar After Carbonation. The control sample (black curve) exhibits higher $CaCO_3$ (Peak C), indicating more carbonation, whereas the biochar-modified sample (red curve, 0.2 wt% biochar) retains more $Ca(OH)_2$ (Peak E), suggesting enhanced hydration, matrix densification, and improved resistance to carbonation.

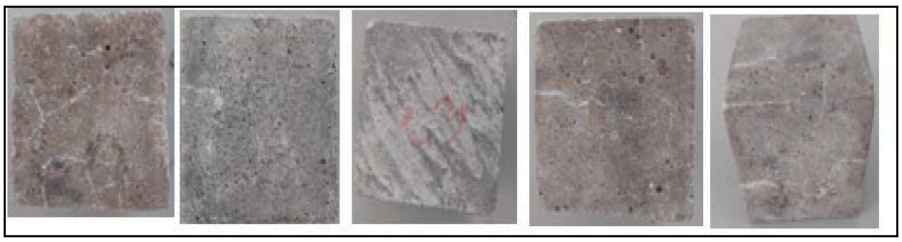

Fig. 19. Surface deterioration of mortar after 100 freeze-thaw cycles with increasing biochar content (0 % to 0.2 % from left to right). Minimal damage is observed at 0.1 % biochar, indicating optimal resistance.

thaw resistance by providing additional moisture during hydration. Biochar's porous structure absorbs water during mixing and gradually releases it, sustaining hydration and promoting C-S-H formation, which densifies the matrix and refines pore structure [101]. This reduces the volume of freezable water and internal stress caused by ice formation, thereby minimizing surface cracking and scaling. Some other relevant studies also show that internal curing in cementitious materials reduces freeze-thaw damage through better hydration and reduced permeability [102]. At 0.15 % biochar, surface cracking reappears, indicating a decline in performance beyond the optimal dosage. The 0.2 % biochar specimen shows increased damage and deformation, suggesting excessive biochar negatively impacts freeze-thaw durability. These findings align with studies indicating that low biochar dosages (e.g., 0.1 %) improve durability by reducing porosity and enhancing matrix densification, while higher amounts may weaken the structure by altering the pore network.

Mass loss after 100 cycles of freeze and thaw is presented in Fig. 20. The results indicate that incorporating biochar into cement-sand mortar enhances its resistance to freezing and thawing cycles. The control sample exhibited the highest mass loss (~1.1 %). As biochar content increased to 0.05 % and 0.1 %, mass loss decreased sharply to ~0.3–0.4 %, suggesting that these dosages optimize freeze-thaw resistance by refining pore structure and reducing water permeability. However, at higher biochar contents (0.15–0.2 %), mass loss slightly increased (~0.4–0.8 %), likely due to excessive porosity or agglomeration effects, though performance remained superior to the control. These findings highlight that 0.1 % P. Juliflora biochar is the most effective dosage for minimizing freeze-thaw damage, while higher concentrations, though still beneficial, may introduce microstructural trade-offs. The results underscore biochar's potential as a sustainable additive for improving mortar durability in cold climates.

The residual compressive strength after 100 cycles of freeze and thaw is shown in Fig. 21.

The results reveal a trend where biochar enhances freeze-thaw resistance in mortar. The control sample (0 % biochar) exhibits the highest strength loss (residual strength: 89.9 %), while the addition of 0.1 % biochar maximizes durability, retaining 93.8 % of its compressive strength. This improvement is likely due to biochar's pore-refining effect, which reduces water penetration and ice formation damage. At higher dosages (0.15–0.2 %), residual strength remains superior to the control (93.7–93.2 %) but shows a slight decline compared to 0.1 %, suggesting a threshold for optimal pore structure modification. These findings highlight biochar's potential as a sustainable additive for cold-weather concrete applications, with 0.1 % emerging as the most effective dosage.

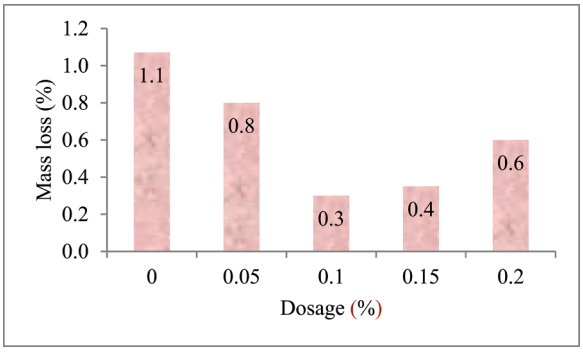

Fig. 20. This figure shows the mass loss of cement-sand mortar with varying biochar content after 100 freeze-thaw cycles. The lowest mass loss (~0.3 %) occurs at 0.1 % biochar, suggesting optimal pore refinement. Higher doses (0.15–0.2 %) slightly reduce effectiveness.

4.10. Thermal resistance

In cementitious materials, water exists in several distinct forms, each with different binding energies and roles in the material's structure. The release of these water types at elevated temperatures significantly contributes to mass loss and can affect the material's mechanical and physical properties [103]. The mass loss results after exposure to a temperature of 450 °C are presented in Fig. 22.

Mass loss trends reveal that biochar dosage non-linearly influences the thermal stability of cementitious mortar, with the peak mass loss (3.62 %) occurring at 0.1 % biochar. Biochar appears to exhibit a dual effect: at lower dosages (≤0.1 %), it may enhance dehydration by creating channels that facilitate moisture escape, leading to increased mass loss. In contrast, at higher dosages (>0.1 %), biochar may serve as a thermal barrier—either by slowing heat transfer or adsorbing moisture—thereby reducing mass loss. Similar behavior has been observed with other porous additives. For instance, Expanded Perlite (EP) at low contents (~5–10 %) increases evaporable water due to its high porosity, resulting in greater mass loss upon heating [104]. However, at higher dosages (>15 %), EP acts as an insulator, limiting heat penetration and delaying hydrate decomposition. Comparable roles have also been reported for Silica Aerogel (SA) [105] and Recycled Glass Foam (RGF) [106].

Fig. 23 shows the relative residual compressive strength of the specimens after a temperature exposure of 450 °C. It can be observed that thermal exposure leads to a decrease in strength for both the control and biochar-containing samples. However, the samples incorporating biochar revealed greater resistance to thermal damage compared to the control. The highest relative residual strength, 87.16 %, was observed in the specimen with 0.1 wt% biochar. A slight decline in strength was noted in samples with biochar content above this percentage. During the heating process, both free water and chemically bound water in the cement matrix are converted into steam, which attempts to escape through the pore structure. This generates internal stresses within the cement composites. Biochar, due to its inherently porous nature, effectively mitigates these stresses by allowing the steam to dissipate through its network of pores. This mechanism contributes to the enhanced compressive strength observed in biochar-based cement mortar specimens under thermal exposure. However, at higher dosages (>0.1 wt%), biochar can also trap moisture and internal steam, increasing internal pressure and potentially causing microcracking or disrupting hydration product stability. Additionally, excessive porosity and particle

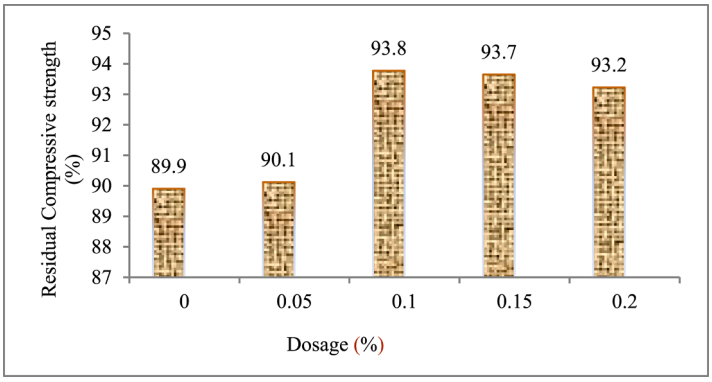

Fig. 21. This figure shows the residual compressive strength (%) of cement-sand mortar after 100 freeze-thaw cycles, with biochar content increasing from 0 % to 0.2 % (left to right). The results indicate that biochar incorporation mitigates strength loss, with optimal performance observed at 0.1 % biochar (93.8 % residual strength).

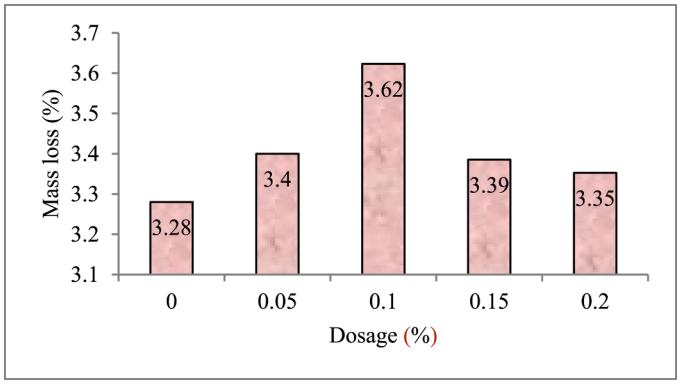

Fig. 22. This Figure displays comparative mass loss of cementitious mortars with varying biochar dosages (0–0.2 %) post-exposure to 450 °C.

agglomeration can weaken the matrix, leading to lower residual compressive strength.

Fig. 24 shows the relative residual flexural strength of the specimens after a temperature exposure of 450 °C.

The observed trend in flexural strength under elevated temperature differs slightly from those of mass loss and residual compressive strength. Mass loss primarily reflects moisture evaporation and thermal degradation of the matrix, which directly impacts compressive strength by affecting cohesion and microstructural integrity. Consequently, the trend in residual compressive strength more closely follows that of mass loss.

However, flexural strength is also influenced by microstructural features such as improved bonding, crack bridging, and surface toughening, which can mitigate damage even when mass loss is comparatively lower [71]. This explains the peak in flexural strength observed at 0.15 wt% biochar, despite higher mass loss and slightly reduced compressive strength at this dosage.

Under compressive loading, the presence of excess biochar beyond the optimal 0.1 wt% may introduce weak zones or reduce the overall packing density due to its porous and low-density nature, leading to a marginal decline in strength. In contrast, under flexural loading conditions, biochar contributes to crack deflection and controls crack width, especially near the tensile surface, which results in a net strengthening effect even at slightly higher dosages. These findings suggest that the mechanical response of biochar-modified mortar under thermal stress is mode-dependent, with optimal performance in compression at 0.1 wt% and in flexure at 0.15 wt%.

4.11. Ecological and economic implications

P. juliflora, though introduced globally for land rehabilitation and resource use, has become a highly invasive species in many arid and semi-arid regions. Its rapid spread, driven by prolific seeding and regeneration, has led to ecosystem degradation and displacement of native flora, prompting interest in sustainable management through productive utilization such as biochar production [107].

Economically, P. juliflora is widely available and fast-growing, which supports a reliable biomass supply [108]. However, industrial-scale implementation may face challenges related to harvesting logistics, transportation from remote growth areas, and

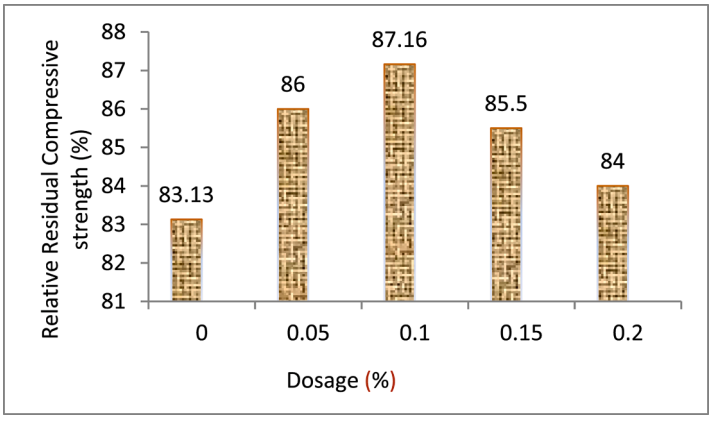

Fig. 23. Relative residual compressive strength of cement mortar with varying biochar dosages after thermal exposure of 450 °C. Strength peaks at 0.1 wt% biochar (87.16 %), suggesting optimal thermal resistance. Beyond this point, a slight decline is observed, likely due to excess porosity or particle agglomeration.

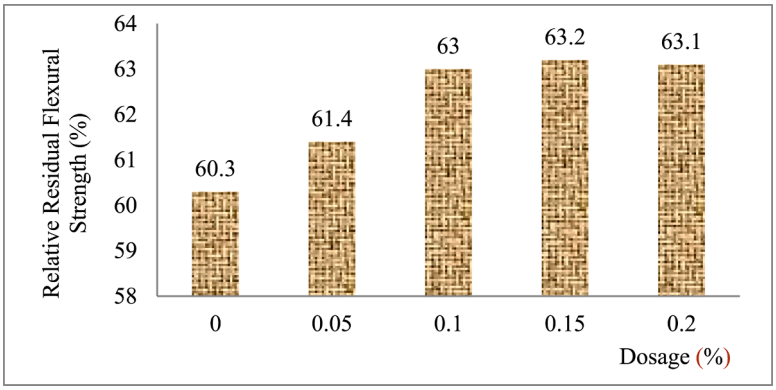

Fig. 24. Relative residual flexural strength of cement mortar with varying biochar dosages after thermal exposure at 450 °C. Strength increases steadily with biochar content, peaking at 0.15 wt% (63.2 %), then slightly tapering off. This suggests that crack-bridging and pore-filling effects of biochar are more influential in bending than in compression.

consistent quality control during pyrolysis. The cost of processing, particularly ensuring uniform particle size, optimized carbonization temperature, and safe handling of emissions may influence its competitiveness compared to conventional supplementary cementitious materials. Additionally, supply chain constraints or lack of centralized biochar production infrastructure could pose barriers to widespread use.

To overcome these hurdles, decentralized, small-scale pyrolysis units near biomass-rich regions could be a viable solution, reducing transport costs and supporting local economies [109]. Government incentives, regulatory support for waste-to-resource conversion, and further techno-economic feasibility studies would be instrumental in promoting the industrial adoption of P. juliflora biochar in sustainable construction applications.

4.12. Future research directions

This study establishes a foundation for utilizing P. juliflora biochar as a value-added material in cementitious composites, offering both technical and environmental advantages. Future research should expand on these findings by assessing the performance of P. juliflora biochar in blended cements, alkali-activated systems, and specialized concrete applications such as self-compacting or lightweight concrete, particularly in alignment with global green building certification systems like LEED (Leadership in Energy and Environmental Design) and BREEAM (Building Research Establishment Environmental Assessment Method) [110]. Investigations into its potential to improve indoor air quality, enhance thermal insulation, and reduce embodied carbon could contribute to achieving credits within these frameworks, further supporting sustainability objectives in the construction industry [111].

Furthermore, P. juliflora biochar presents a globally relevant solution by transforming an ecologically invasive biomass, prevalent in arid and semi-arid regions, into a functional, low-impact construction material. This approach aligns with key United Nations Sustainable Development Goals (SDGs), including SDG 11 (Sustainable Cities and Communities), SDG 12 (Responsible Consumption and Production), and SDG 13 (Climate Action). It also supports Intergovernmental Panel on Climate Change (IPCC) recommendations for mitigating cement-related emissions through material innovation and carbon-efficient design. Future studies should incorporate life cycle assessments (LCA), techno-economic analyses, and exploration of decentralized pyrolysis systems to evaluate the scalability and circularity of P. juliflora biochar across diverse regional contexts. Such efforts can accelerate the transition toward a low-carbon, resource-efficient construction paradigm on a global scale.

5. Conclusions

Prosopis Juliflora, commonly known as mesquite, is native to South America. This tree was intentionally introduced to various parts of the world due to its numerous benefits, including adaptability to desert environments, fast growth, use as a fuelwood source, provision of food for livestock and humans, shade provision, soil stabilization through its extensive root system, and the enhancement of soil fertility through atmospheric nitrogen fixation. Despite these advantages, P. Juliflora is considered invasive in many regions, where it competes with native species and reduces crop areas. To control its spread, the plant is often dumped or burned, leading to the emission of greenhouse gases. This study aimed to extract biochar from P. Juliflora and investigate its potential use in cementitious mortar. The following conclusions were drawn from the research:

1. Biochar extracted from P. Juliflora is rich in carbon, retaining 83 % carbon as confirmed by EDX analysis, making it an effective carbon sink.
2. The extracted biochar has a rough, porous, and elongated structure, which enhances its suitability for use in cement-based composites.
3. The inclusion of P. Juliflora biochar in cement mortar improves compressive strength, with a maximum increase of 11.5 % compared to the control mortar at a 0.1 % addition. Further biochar additions result in a decrease in strength, but it remains higher than that of the control mortar.
4. The addition of P. Juliflora biochar also improves flexural strength, with a maximum increase of 21 % compared to the control specimen at 90 days. Strength declines with higher biochar content but stays above the control levels.
5. The incorporation of P. Juliflora biochar improves the density of the cement mortar, with the highest density observed at a 0.1 % biochar addition. Density decreases with further increases in biochar content.
6. Porosity is reduced with the inclusion of P. Juliflora biochar, with the lowest porosity observed at 0.1 % biochar addition. Porosity increases with higher biochar dosages.
7. The carbonation test demonstrates that biochar effectively reduces carbonation depth, with 0.1 wt% being the optimal dosage for minimizing CO_2 penetration. Beyond this concentration, increased porosity slightly diminishes the densification effect, though biochar samples still outperform the control.
8. Thermal test revealed that the biochar acted as a dehydration promoter at lower dosages ($\leq$0.1 wt%) and as a thermal insulator in cementitious mortars at higher dosages (>0.1 wt%).

9. The thermal test results demonstrate that while both residual compressive and flexural strengths decrease with temperature exposure, biochar-enhanced specimens, particularly those with 0.1 wt% biochar, show better thermal resistance, with flexural strength benefiting from improved microstructural enhancements despite slight reductions in compressive strength at higher biochar contents.
10. A 0.1 % P. Juliflora biochar content by weight of cement is identified as the optimal dosage for enhancing the performance of cement mortar.

CRediT authorship contribution statement

Israr Ahmad: Resources, Methodology, Investigation, Formal analysis, Data curation. **Faheem Butt:** Validation, Supervision, Resources, Project administration, Conceptualization. **Anwar Khitab:** Writing – review & editing, Writing – original draft, Validation, Supervision, Project administration, Formal analysis, Conceptualization.

Declaration of competing interest

The authors have declared no conflict of interest

Data availability

No data was used for the research described in the article.

References

[1] K.L. Scrivener, V.M. John, E.M. Gartner, Eco-efficient cements: potential economically viable solutions for a low-CO2 cement-based materials industry, Cem. Concr. Res. 114 (2018) 2–26, https://doi.org/10.1016/j.cemconres.2018.03.015.

[2] T.A.-S.S. A. Danish, M. Salim, U.An Materials, Trends and developments in green cement "A sustainable approach," Core.Ac.UkA Danish, MU Salim, T AhmedSustainable Struct Mater. Int. J. (2019) https://doi.org/10.26392/SSM.2019.02.01.045, 2019•core.Ac.Uk. (n.d.)

[3] World Economic Forum, Net-zero industry tracker 2023, 91–93 route de la Capite CH-1223 Cologny/Geneva Switzerland, 2023. https://www3.weforum.org/docs/WEF_Net_Zero_Tracker_2023_REPORT.pdf.

[4] Y. Zhang, J. Zhang, W. Luo, J. Wang, J. Shi, H. Zhuang, Y. Wang, Effect of compressive strength and chloride diffusion on life cycle CO2 assessment of concrete containing supplementary cementitious materials, J. Clean. Prod. 218 (2019) 450–458, https://doi.org/10.1016/j.jclepro.2019.01.335.

[5] D.O. Oyejobi, A.A. Firoozi, D.B. Fernández, S. Avudaiappan, Integrating circular economy principles into concrete technology: enhancing sustainability through industrial waste utilization, Results Eng. 24 (2024) 102846, https://doi.org/10.1016/j.rineng.2024.102846.

[6] A. Sirico, P. Bernardi, B. Belletti, A. Malcevschi, E. Dalcanale, I. Domenichelli, P. Fornoni, E. Moretti, Mechanical characterization of cement-based materials containing biochar from gasification, Constr. Build. Mater. 246 (2020) 118490, https://doi.org/10.1016/j.conbuildmat.2020.118490.

[7] M.T. Arshad, S. Ahmad, A. Khitab, A. Hanif, Synergistic use of fly ash and silica fume to produce high-strength self-compacting cementitious composites, Crystals 11 (2021) 915, https://doi.org/10.3390/cryst11080915.

[8] M. Ebrahimi, S. Gholipour, G. Mostafaii, F. Yousefian, Biochar-amended food waste compost: a review of properties, Results Eng. 24 (2024) 103118, https://doi.org/10.1016/j.rineng.2024.103118.

[9] W. Nasir Khan, S.G.H. Kazmi, A. Khitab, Effect of bio-char of Santa Maria feverfew plant on physical properties of fresh mortar, in: CSCE 2023, MDPI, Basel Switzerland, 2023: p. 4. https://doi.org/10.3390/engproc2023044004.

[10] M. Arif, T. Jan, M. Riaz, S. Fahad, M. Adnan, K.A. Amanullah, I.A. Mian, B. Khan, F. Rasul, Biochar; a remedy for Climate change, Environ. Clim. Plant Veg. Growth (2020) 151–171, https://doi.org/10.1007/978-3-030-49732-3_8.

[11] G. Agegnehu, A. Srivastava, M.I. Bird, The role of biochar and biochar-compost in improving soil quality and crop performance: a review, Appl. Soil Ecol. 119 (2017) 156–170, https://doi.org/10.1016/j.apsoil.2017.06.008.

[12] K. Qian, A. Kumar, H. Zhang, D. Bellmer, R. Huhnke, Recent advances in utilization of biochar, Renew. Sustain. Energy Rev. 42 (2015) 1055–1064, https://doi.org/10.1016/j.rser.2014.10.074.

[13] R.K. Mishra, S. Chinnam, A. Sharma, Thermocatalytic pyrolysis of low-value waste biomass: thermal decomposition, kinetics behaviour, and biochar characterization, Results Eng. 25 (2025) 104210, https://doi.org/10.1016/j.rineng.2025.104210.

[14] N. Rambhatla, T.F. Panicker, R.K. Mishra, S.K. Manjeshwar, A. Sharma, Biomass pyrolysis for biochar production: study of kinetics parameters and effect of temperature on biochar yield and its physicochemical properties, Results Eng. 25 (2025) 103679, https://doi.org/10.1016/j.rineng.2024.103679.

[15] N. Bolan, S.A. Hoang, J. Beiyuan, S. Gupta, D. Hou, A. Karakoti, S. Joseph, S. Jung, K.H. Kim, M.B. Kirkham, H.W. Kua, M. Kumar, E.E. Kwon, Y.S. Ok, V. Perera, J. Rinklebe, S.M. Shaheen, B. Sarkar, A.K. Sarmah, B.P. Singh, G. Singh, D.C.W. Tsang, K. Vikrant, M. Vithanage, A. Vinu, H. Wang, H. Wijesekara, Y. Yan, S.A. Younis, L. Van Zwieten, Multifunctional applications of biochar beyond carbon storage, Int. Mater. Rev. 67 (2022) 150–200, https://doi.org/10.1080/09506608.2021.1922047.

[16] S. Mona, S.K. Malyan, N. Saini, B. Deepak, A. Pugazhendhi, S.S. Kumar, Towards sustainable agriculture with carbon sequestration, and greenhouse gas mitigation using algal biochar, Chemosphere 275 (2021) 129856, https://doi.org/10.1016/j.chemosphere.2021.129856.

[17] R.R. Tan, Data challenges in optimizing biochar-based carbon sequestration, Renew. Sustain. Energy Rev. 104 (2019) 174–177, https://doi.org/10.1016/j.rser.2019.01.032.

[18] J.H. Park, Y.U. Kim, J. Jeon, B.Y. Yun, Y. Kang, S. Kim, Analysis of biochar-mortar composite as a humidity control material to improve the building energy and hygrothermal performance, Sci. Total Environ. 775 (2021) 145552, https://doi.org/10.1016/j.scitotenv.2021.145552.

[19] S. Yang, S. Wi, J. Lee, H. Lee, S. Kim, Biochar-red clay composites for energy efficiency as eco-friendly building materials: thermal and mechanical performance, J. Hazard. Mater. 373 (2019) 844–855, https://doi.org/10.1016/j.jhazmat.2019.03.079.

[20] F.R. Vieira, C.M. Romero Luna, G.L.A.F. Arce, I. Ávila, Optimization of slow pyrolysis process parameters using a fixed bed reactor for biochar yield from rice husk, Biomass Bioenergy 132 (2020) 105412, https://doi.org/10.1016/j.biombioe.2019.105412.

[21] A. Akhtar, A.K. Sarmah, Novel biochar-concrete composites: manufacturing, characterization and evaluation of the mechanical properties, Sci. Total Environ. 616–617 (2018) 408–416, https://doi.org/10.1016/j.scitotenv.2017.10.319.

[22] K. Tan, Y. Qin, J. Wang, Evaluation of the properties and carbon sequestration potential of biochar-modified pervious concrete, Constr. Build. Mater. 314 (2022) 125648, https://doi.org/10.1016/j.conbuildmat.2021.125648.

[23] H. Maljaee, R. Madadi, H. Paiva, L. Tarelho, V.M. Ferreira, Incorporation of biochar in cementitious materials: a roadmap of biochar selection, Constr. Build. Mater. 283 (2021) 122757, https://doi.org/10.1016/j.conbuildmat.2021.122757.

[24] D.C.B.D. Santos, R.B.W. Evaristo, R.C. Dutra, P.A.Z. Suarez, E.A. Silveira, G. F. Ghesti, Advancing biochar applications: a review of production processes, analytical methods, decision criteria, and pathways for scalability and certification, Sustainability 17 (2025) 2685, https://doi.org/10.3390/su17062685.

[25] H. Zhang, Y. Cheng, Y. Zhong, J. Ni, R. Wei, W. Chen, Roles of biochars' properties in their water-holding capacity and bound water evaporation: quantitative importance and controlling mechanism, Biochar 6 (2024) 30, https://doi.org/10.1007/s42773-024-00317-2.

[26] Y. Ling, X. Wu, K. Tan, Z. Zou, Effect of biochar dosage and fineness on the mechanical properties and durability of concrete, Materials 16 (2023) 2809, https://doi.org/10.3390/ma16072809.

[27] X. Lin, W. Li, Y. Guo, W. Dong, A. Castel, K. Wang, Biochar-cement concrete toward decarbonisation and sustainability for construction: characteristic, performance and perspective, J. Clean. Prod. 419 (2023) 138219, https://doi.org/10.1016/j.jclepro.2023.138219.

[28] S. Gupta, H.W. Kua, S.D. Pang, Biochar-mortar composite: manufacturing, evaluation of physical properties and economic viability, Constr. Build. Mater. 167 (2018) 874–889, https://doi.org/10.1016/j.conbuildmat.2018.02.104.

[29] W.C. Choi, H. Do Yun, J.Y. Lee, Mechanical properties of mortar containing biochar from pyrolysis, J. Korea Inst. Struct. Maint. Insp. 16 (2012) 67–74, https://doi.org/10.11112/jksmi.2012.16.3.067.

[30] S. Gupta, H.W. Kua, C.Y. Low, Use of biochar as carbon sequestering additive in cement mortar, Cem. Concr. Compos. 87 (2018) 110–129, https://doi.org/10.1016/j.cemconcomp.2017.12.009.

[31] A. Sirico, P. Bernardi, C. Sciancalepore, F. Vecchi, A. Malcevschi, B. Belletti, D. Milanese, Biochar from wood waste as additive for structural concrete, Constr. Build. Mater. 303 (2021) 124500, https://doi.org/10.1016/j.conbuildmat.2021.124500.

[32] Y.U. Kim, B.Y. Yun, J. Nam, J.Y. Choi, S. Wi, S. Kim, Evaluation of thermal properties of phase change material-integrated artificial stone according to biochar loading content, Constr. Build. Mater. 305 (2021) 124682, https://doi.org/10.1016/j.conbuildmat.2021.124682.

[33] S. Gupta, S. Muthukrishnan, H.W. Kua, Comparing influence of inert biochar and silica rich biochar on cement mortar – Hydration kinetics and durability under chloride and sulfate environment, Constr. Build. Mater. 268 (2021) 121142, https://doi.org/10.1016/j.conbuildmat.2020.121142.

[34] S. Tayyab, A. Khitab, A. Iftikhar, R.B.N. Khan, M.S. Kirgiz, Manufacturing of high-performance light-weight mortar through addition of biochars of millet and maize, Waste Dispos. Sustain. Energy 5 (2023) 97–111, https://doi.org/10.1007/s42768-023-00135-5.

[35] A. Iftikhar, R. Arsalan Khushnood, A. Khitab, S. Ahmad, Improved fracture response and electromagnetic interference shielding effectiveness of cementitious composites incorporating pyrolytic bagasse fibers and pine needles, Constr. Build. Mater. 370 (2023) 130722, https://doi.org/10.1016/j.conbuildmat.2023.130722.

[36] R. Mensah, V. Shanmugam, S. Narayanan, N. Razavi, A. Ulfberg, T. Blanksvärd, F. Sayahi, P. Simonsson, B. Reinke, M. Försth, G. Sas, D. Sas, O. Das, Biochar-

added cementitious materials—a review on mechanical, thermal, and environmental properties, Sustainability 13 (2021) 9336, https://doi.org/10.3390/su13169336.
[37] Y. Zhang, Y. Maierdan, T. Guo, B. Chen, S. Fang, L. Zhao, Biochar as carbon sequestration material combines with sewage sludge incineration ash to prepare lightweight concrete, Constr. Build. Mater. 343 (2022) 128116, https://doi.org/10.1016/j.conbuildmat.2022.128116.
[38] N. Pasiecznik, Prosopis-pest or providence, weed or wonder tree? Eur. Trop. For. Res. Netw. Newsl. 28 (1999) 12–14.
[39] Z.H. Mehari, The invasion of Prosopis juliflora and Afar pastoral livelihoods in the Middle Awash area of Ethiopia, Ecol. Process. 4 (2015) 13, https://doi.org/10.1186/s13717-015-0039-8.
[40] E. Mwangi, B. Swallow, Prosopis juliflora invasion and rural livelihoods in the Lake Baringo area of Kenya, Conserv. Soc. 6 (2008) 130–140.
[41] S. Rettberg, D. Müller-Mahn, Human–environment interactions: the invasion of Prosopis Juliflora in the drylands of Northeast Ethiopia. Changing Deserts-Integrating People and their Environments, THE WHITE HORSE PRESS, The Old Vicarage, Winwick, Cambridgeshire, PE28 5PN, UK, 2012, pp. 297–316.
[42] H.M. Alkharabsheh, R. Mwadalu, B. Mochoge, B. Danga, M.A. Raza, M. F. Seleiman, N. Khan, H. Gitari, Revitalizing the biochemical soil properties of degraded coastal soil using Prosopis juliflora Biochar, Life (Basel) 13 (2023), https://doi.org/10.3390/life13102098.
[43] S. Jayaprakash, V. Deivasigamani, G. Ravindran, Influence of Prosopis juliflora ash in mechanical properties of concrete, Mater. Today Proc. 80 (2023) 1168–1172, https://doi.org/10.1016/j.matpr.2022.12.127.
[44] M.I. Al-Wabel, A. Al-Omran, A.H. El-Naggar, M. Nadeem, A.R.A. Usman, Pyrolysis temperature induced changes in characteristics and chemical composition of biochar produced from conocarpus wastes, Bioresour. Technol. 131 (2013) 374–379, https://doi.org/10.1016/j.biortech.2012.12.165.
[45] C. Zhao, X. Liu, A. Chen, J. Chen, W. Lv, X. Liu, Characteristics evaluation of biochar produced by pyrolysis from waste hazelnut shell at various temperatures, Energy Sources, Part A Recover. Util. Environ. Eff. 46 (2024) 7403–7413, https://doi.org/10.1080/15567036.2020.1754530.
[46] H. Maljaee, H. Paiva, R. Madadi, L.A.C. Tarelho, M. Morais, V.M. Ferreira, Effect of cement partial substitution by waste-based biochar in mortars properties, Constr. Build. Mater. 301 (2021) 124074, https://doi.org/10.1016/j.conbuildmat.2021.124074.
[47] S. Gupta, A. Kashani, Utilization of biochar from unwashed peanut shell in cementitious building materials – effect on early age properties and environmental benefits, Fuel Process. Technol. 218 (2021) 106841, https://doi.org/10.1016/j.fuproc.2021.106841.
[48] A.Y. Elnour, A.A. Alghyamah, H.M. Shaikh, A.M. Poulose, S.M. Al-Zahrani, A. Anis, M.I. Al-Wabel, Effect of pyrolysis temperature on biochar microstructural evolution, physicochemical characteristics, and its influence on biochar/polypropylene composites, Appl. Sci. 9 (2019) 1149, https://doi.org/10.3390/app9061149.
[49] S. Gupta, H.W. Kua, H.J. Koh, Application of biochar from food and wood waste as green admixture for cement mortar, Sci. Total Environ. 619–620 (2018) 419–435, https://doi.org/10.1016/j.scitotenv.2017.11.044.
[50] S. Wijitkosum, P. Jiwnok, Elemental composition of biochar obtained from agricultural waste for soil amendment and carbon sequestration, Appl. Sci. 9 (2019) 3980, https://doi.org/10.3390/app9193980.
[51] L. Wang, L. Chen, D.C.W. Tsang, B. Guo, J. Yang, Z. Shen, D. Hou, Y.S. Ok, C. S. Poon, Biochar as green additives in cement-based composites with carbon dioxide curing, J. Clean. Prod. 258 (2020) 120678, https://doi.org/10.1016/j.jclepro.2020.120678.
[52] A. Akhtar, A.K. Sarmah, Strength improvement of recycled aggregate concrete through silicon rich char derived from organic waste, J. Clean. Prod. 196 (2018) 411–423, https://doi.org/10.1016/j.jclepro.2018.06.044.
[53] ASTM C1437-20, standard test method for flow of hydraulic cement mortar, West Conshohocken, PA, 19428-2959 USA, 2020.
[54] ASTM, D854 - standard test methods for specific gravity of soil solids by water pycnometer, Astm D854. 2458000 (2000) 1–7. https://doi.org/10.1520/D0854-10.2.
[55] ASTM D570-22, test method for water absorption of plastics, (2022). https://doi.org/10.1520/D0570-22.
[56] ASTM, ASTM C348. Standard test method for flexural strength of hydraulic-cement Mortars1, Annu. B. ASTM Stand. 04 (1998) 2–7, https://doi.org/10.1520/C0348-14.2.
[57] ASTM C349-08, standard test method for compressive strength of hydraulic-cement mortars (Using Portions of Prisms Broken in Flexure), West Conshohocken, PA, 19428-2959 USA, 2008. https://doi.org/10.1520/C0349-08.2.
[58] M.G. Beltrán, A. Barbudo, F. Agrela, J.R. Jiménez, J. de Brito, Mechanical performance of bedding mortars made with olive biomass bottom ash, Constr. Build. Mater. 112 (2016) 699–707, https://doi.org/10.1016/j.conbuildmat.2016.02.065.
[59] RILEM TC 56-MHM, CPC-18 measurement of hardened concrete carbonation depth, Mater. Struct. 21 (1996) 453–456.
[60] BS EN 14630:2006, products and systems for the protection and repair of concrete structures - test methods - determination of carbonation depth in hardened concrete by the phenolphthalein method, 389 Chiswick High Road London BSI UK, 2006.
[61] Astm C666/C666M, standard test method for resistance of concrete to rapid freezing and thawing, ASTM int. West Conshohocken, PA. 03 (2003) 1–6.
[62] S. Navaratnam, H. Wijaya, P. Rajeev, P. Mendis, K. Nguyen, Residual stress-strain relationship for the biochar-based mortar after exposure to elevated temperature, Case Stud. Constr. Mater. 14 (2021) e00540, https://doi.org/10.1016/j.cscm.2021.e00540.
[63] A.K. Subhani, M. Nisar, A. Khitab, Improvement of early-age mechanical properties of cement mortar by adding biochar of the Santa Maria feverfew plant. CSCE 2023, MDPI, Basel Switzerland, 2023, p. 7, https://doi.org/10.3390/engproc2023044007.
[64] J. O'Laughlin, K. McElligott, Biochar for environmental management: science and technology, For. Policy Econ. 11 (2009) 535–536, https://doi.org/10.1016/j.forpol.2009.07.001.
[65] E.B. Dayoub, Z. Tóth, G. Soós, A. Anda, Chemical and physical properties of selected biochar types and a few application methods in agriculture, Agronomy 14 (2024) 2540, https://doi.org/10.3390/agronomy14112540.
[66] R. Chintala, T.E. Schumacher, L.M. McDonald, D.E. Clay, D.D. Malo, S. K. Papiernik, S.A. Clay, J.L. Julson, Phosphorus sorption and availability from biochars and soil/biochar mixtures, CLEAN – Soil, Air, Water 42 (2014) 626–634, https://doi.org/10.1002/clen.201300089.
[67] A. Downie, A. Crosky, P. Munroe, Physical properties of biochar. In: Biochar for Environmental Management, Routledge, Taylor & Francis Group, London, 2009, p. 20.
[68] S. Zou, M.L. Sham, J. Xiao, L.M. Leung, J.-X. Lu, C.S. Poon, Biochar-enabled carbon negative aggregate designed by core-shell structure: a novel biochar utilizing method in concrete, Constr. Build. Mater. 449 (2024) 138507, https://doi.org/10.1016/j.conbuildmat.2024.138507.
[69] D. Wang, A. Jantwal, E. Kaynak, G. Sas, O. Das, Promoting internal curing in concrete by replacing sand with sustainable biochar, Case Stud. Constr. Mater. 22 (2025) e04542, https://doi.org/10.1016/j.cscm.2025.e04542.
[70] P. Yu, X. Wang, C. Zheng, M. Deng, Synergetic effect of magnesium oxide expansion additive and biochar on deformation and mechanical properties of concrete, Mag. Concr. Res. 77 (2025) 95–103, https://doi.org/10.1680/jmacr.24.00052.
[71] M.H. Ellahi, M.S. Siddique, S.H. Siddique, H. Ullah, I. Ahmad, A. Khitab, Lantana Camara plant-biochar added cementitious mortar for carbon sequestration: effect on early-age properties, In: Constr. Technol. Archit (2024) 49–56, https://doi.org/10.4028/p-lF8xSk.
[72] A. Aneja, R.L. Sharma, H. Singh, Mechanical and durability properties of biochar concrete, Mater. Today Proc. 65 (2022) 3724–3730, https://doi.org/10.1016/j.matpr.2022.06.371.
[73] M.F. Akhtar, A. Faraz, A. Khitab, Transforming concrete with steel slag: exploring the pores' dual effect for sustainable and high−performance urban construction, Discov. Civ. Eng. 2 (2025) 81, https://doi.org/10.1007/s44290-025-00243-7.
[74] Z. Zhou, J. Wang, K. Tan, Y. Chen, Enhancing biochar impact on the mechanical properties of cement-based mortar: an optimization study using response surface methodology for particle size and content, Sustainability 15 (2023) 14787, https://doi.org/10.3390/su152014787.
[75] M.H. Ellahi, M.S. Siddique, S.H. Siddique, H. Ullah, I. Ahmad, A. Khitab, Lantana Camara plant-biochar added cementitious mortar for carbon sequestration: effect on early-age properties, Construction Technologies and Architecture. Trans Tech Publications Ltd, 13 (2024) pp. 49–56. https://doi.org/10.4028/p-lF8xSk.
[76] W. Xu, Y. Zhang, M. Li, F. Qu, C.S. Poon, X. Zhu, D.C.W. Tsang, Durability and micromechanical properties of biochar in biochar-cement composites under marine environment, J. Clean. Prod. 450 (2024) 141842, https://doi.org/10.1016/j.jclepro.2024.141842.
[77] S. Gupta, H.W. Kua, Carbonaceous micro-filler for cement: effect of particle size and dosage of biochar on fresh and hardened properties of cement mortar, Sci. Total Environ. 662 (2019) 952–962, https://doi.org/10.1016/j.scitotenv.2019.01.269.
[78] S. Li, L. Jin, X. Chen, M. Hu, Y. Geng, K. Li, Y. Liu, Q. Hu, S. Zhang, Effect and mechanisms of biochar particle size and dosage on the hydration process and mechanical properties of cementitious materials, Constr. Build. Mater. 472 (2025) 140931, https://doi.org/10.1016/j.conbuildmat.2025.140931.
[79] S. Aronhime, C. Calcagno, G.H. Jajamovich, H.A. Dyvorne, P. Robson, D. Dieterich, M. Isabel Fiel, V. Martel-Laferriere, M. Chatterji, H. Rusinek, B. Taouli, DCE-MRI of the liver: effect of linear and nonlinear conversions on hepatic perfusion quantification and reproducibility, J. Magn. Reson. Imaging 40 (2014) 90–98, https://doi.org/10.1002/jmri.24341.
[80] S. Singh, K.R. Shekaran, R. Agarwal, V.G. Kalpana, H. Athar, R. Kumar, S. Naik B, Enhancing the strength and durability of mixed biochar-blended mortars after accelerated carbonation curing (ACC), J. Build. Eng. 100 (2025) 111743, https://doi.org/10.1016/j.jobe.2024.111743.
[81] M. Haris Javed, M. Ali Sikandar, W. Ahmad, M. Tariq Bashir, R. Alrowais, M. Bilal Wadud, Effect of various biochars on physical, mechanical, and microstructural characteristics of cement pastes and mortars, J. Build. Eng. 57 (2022) 104850, https://doi.org/10.1016/j.jobe.2022.104850.
[82] S. Ahmad, J.M. Tulliani, G.A. Ferro, R.A. Khushnood, L. Restuccia, P. Jagdale, Crack path and fracture surface modifications in cement composites, Frat. Ed Integr. Strutt. (2015), https://doi.org/10.3221/IGF-ESIS.34.58.
[83] S. Ahmad, R.A. Khushnood, P. Jagdale, J.-M. Tulliani, G.A. Ferro, High performance self-consolidating cementitious composites by using micro carbonized bamboo particles, Mater. Des. 76 (2015) 223–229, https://doi.org/10.1016/j.matdes.2015.03.048.
[84] S. Melais, M.F. Bouali, A. Melaikia, A. Amirat, Effects of coarse sand dosage on the physic-mechanical behavior of sand concrete, Frat. Ed Integr. Strutt. 15 (2021) 151–159, https://doi.org/10.3221/IGF-ESIS.56.12.

[85] X. Jiang, B. Li, J. Li, J. Guo, Study on the properties of different biochar to cement paste, IOP Conf. Ser. Earth Environ. Sci. 526 (2020) 012085, https://doi.org/10.1088/1755-1315/526/1/012085.
[86] M. Gray, M. G.Johnson, M. I.Dragila, M. Kleber, Water uptake in biochars: the roles of porosity and hydrophobicity, Biomass Bioenergy 61 (2014) 196–205, https://doi.org/10.1016/j.biombioe.2013.12.010.
[87] A. Goldman, A. Bentur, Properties of cementitious systems containing silica fume or nonreactive microfillers, Adv. Cem. Mater. 1 (1994) 209–215, https://doi.org/10.1016/1065-7355(94)90026-4.
[88] N.M. Ali, H. Alanazi, Uncertainty quantification of the flexural strengthening of RC beams with UHPC using improved metaheuristic algorithm, Ain Shams Eng. J. 15 (2024) 102713, https://doi.org/10.1016/j.asej.2024.102713.
[89] L. Restuccia, G.A. Ferro, Nanoparticles from food waste: a “green” future for traditional building materials, (2016). https://doi.org/10.21012/fc9.276.
[90] S. Diamond, D. Bonen, Microstructure of hardened cement paste—a new interpretation, J. Am. Ceram. Soc. 76 (1993) 2993–2999, https://doi.org/10.1111/j.1151-2916.1993.tb06600.x.
[91] R.A. Khushnood, S. Ahmad, P. Savi, J.M. Tulliani, M. Giorcelli, G.A. Ferro, Improvement in electromagnetic interference shielding effectiveness of cement composites using carbonaceous nano/micro inerts, Constr. Build. Mater. 85 (2015) 208–216, https://doi.org/10.1016/j.conbuildmat.2015.03.069.
[92] A. Khitab, R.B.N. Khan, U. Safeer, Enhancement of concrete performance by using compound mixture of waste pottery and red brick powders, Int. J. Mason. Res. Innov. 1 (2024), https://doi.org/10.1504/IJMRI.2024.10062676.
[93] Q. Qiu, A state-of-the-art review on the carbonation process in cementitious materials: fundamentals and characterization techniques, Constr. Build. Mater. 247 (2020) 118503, https://doi.org/10.1016/j.conbuildmat.2020.118503.
[94] A. Morandeau, M. Thiéry, P. Dangla, Investigation of the carbonation mechanism of CH and C-S-H in terms of kinetics, microstructure changes and moisture properties, Cem. Concr. Res. 56 (2014) 153–170, https://doi.org/10.1016/j.cemconres.2013.11.015.
[95] K. Tan, Y. Qin, T. Du, L. Li, L. Zhang, J. Wang, Biochar from waste biomass as hygroscopic filler for pervious concrete to improve evaporative cooling performance, Constr. Build. Mater. 287 (2021) 123078, https://doi.org/10.1016/j.conbuildmat.2021.123078.
[96] S. Gupta, H.W. Kua, C.Y. Low, Use of biochar as carbon sequestering additive in cement mortar, Cem. Concr. Compos. 87 (2018) 110–129, https://doi.org/10.1016/j.cemconcomp.2017.12.009.
[97] K.-H. Tan, T.-Y. Wang, Z.-H. Zhou, Y.-H. Qin, Biochar as a partial cement replacement material for developing sustainable concrete: an overview, J. Mater. Civ. Eng. 33 (2021), https://doi.org/10.1061/(ASCE)MT.1943-5533.0003987.
[98] M. Ahmad, A.U. Rajapaksha, J.E. Lim, M. Zhang, N. Bolan, D. Mohan, M. Vithanage, S.S. Lee, Y.S. Ok, Biochar as a sorbent for contaminant management in soil and water: a review, Chemosphere 99 (2014) 19–33, https://doi.org/10.1016/j.chemosphere.2013.10.071.
[99] A. Pawar, N.L. Panwar, A comparative study on morphology, composition, kinetics, thermal behaviour and thermodynamic parameters of Prosopis Juliflora and its biochar derived from vacuum pyrolysis, Bioresour. Technol. Rep. 18 (2022) 101053, https://doi.org/10.1016/j.biteb.2022.101053.
[100] S. Sivaraman, S.R. Shanmugam, P. Venkatachalam, R. Shanmugam, A. Chan Basha, N.M.C. Saady, Effect of pretreatment type on the physico-chemical properties of activated carbons derived from an invasive weed Prosopis juliflora: potential applications, Mater. Res. Express. 12 (2025) 015601, https://doi.org/10.1088/2053-1591/ada5c4.
[101] Y. Qin, X. Pang, K. Tan, T. Bao, Evaluation of pervious concrete performance with pulverized biochar as cement replacement, Cem. Concr. Compos. 119 (2021) 104022, https://doi.org/10.1016/j.cemconcomp.2021.104022.
[102] H. Chen, Y. Cao, Y. Liu, Y. Qin, L. Xia, Enhancing the durability of concrete in severely cold regions: mix proportion optimization based on machine learning, Constr. Build. Mater. 371 (2023) 130644, https://doi.org/10.1016/j.conbuildmat.2023.130644.
[103] E.U. Khan, R.A. Khushnood, W.L. Baloch, Spalling sensitivity and mechanical response of an ecofriendly sawdust high strength concrete at elevated temperatures, Constr. Build. Mater. 258 (2020) 119656, https://doi.org/10.1016/j.conbuildmat.2020.119656.
[104] Z. Lu, A. Hanif, C. Lu, K. Liu, G. Sun, Z. Li, A novel lightweight cementitious composite with enhanced thermal insulation and mechanical properties by extrusion technique, Constr. Build. Mater. 163 (2018) 446–449, https://doi.org/10.1016/j.conbuildmat.2017.12.130.
[105] Y. Wang, J. Huang, D. Wang, Y. Liu, Z. Zhao, J. Liu, Experimental investigation on thermal conductivity of aerogel-incorporated concrete under various hygrothermal environment, Energy 188 (2019) 115999, https://doi.org/10.1016/j.energy.2019.115999.
[106] W.S. Mustafa, J. Szendefy, B. Nagy, Thermal performance of foam glass aggregate at different compaction ratios, Buildings 13 (2023) 1844, https://doi.org/10.3390/buildings13071844.
[107] S. Gupta, R. Vinayak More, A. Yadav, Characterisation of biochar and estimation of net GHG emissions from Prosopis Juliflora biomass for soil and solid fuel application, Mater. Today Proc. (2023), https://doi.org/10.1016/j.matpr.2023.03.291.
[108] R.T. Shackleton, D.C. Le Maitre, N.M. Pasiecznik, D.M. Richardson, Prosopis: a global assessment of the biogeography, benefits, impacts and management of one of the world’s worst woody invasive plant taxa, AoB Plants 6 (2014), https://doi.org/10.1093/aobpla/plu027.
[109] PYRAGRAF Project, decentralized pyrolytic conversion of agriculture and forestry wastes towards local circular value chains and sustainability, (2023). https://www.pyragraf.eu/en/home/ (accessed 29 June 2025).
[110] M.B. Subhani, A. Khitab, Carbon footprint reduction in mid-rise buildings: analysis, design, and LCA-based evaluation of alternate steel slag aggregates in concrete, Discov. Civ. Eng. 2 (2025) 119, https://doi.org/10.1007/s44290-025-00276-y.
[111] A.A. Firoozi, A.A. Firoozi, D.O. Oyejobi, S. Avudaiappan, E.S. Flores, Emerging trends in sustainable building materials: technological innovations, enhanced performance, and future directions, Results Eng. 24 (2024) 103521, https://doi.org/10.1016/j.rineng.2024.103521.